



1 Highly oxygenated organic molecules (HOM) formation in the 2 isoprene oxidation by NO₃ radical

3 Defeng Zhao^{1,2}, Iida Pullinen^{2,*}, Hendrik Fuchs², Stephanie Schrade², Rongrong Wu², Ismail-Hakki Acir^{2,b}, Ralf Tillmann²,
4 Franz Rohrer², Jürgen Wildt², Yindong Guo¹, Astrid Kiendler-Scharr², Andreas Wahner², Sungah Kang², Luc Vereecken²,
5 Thomas F. Mentel²

6 ¹Department of Atmospheric and Oceanic Sciences & Institute of Atmospheric Sciences, Fudan University, 200438,
7 Shanghai, China;

8 ²Institute of Energy and Climate Research, IEK-8: Troposphere, Forschungszentrum Jülich, 52425, Jülich, Germany

9 ^aNow at: Department of Applied Physics, University of Eastern Finland, Kuopio, 7021, Finland.

10 ^bNow at: Institute of Nutrition and Food Sciences, University of Bonn, Bonn, 53115, Germany;

11 *Correspondence to:* Thomas F. Mentel (t.mentel@fz-juelich.de)

12 Abstract

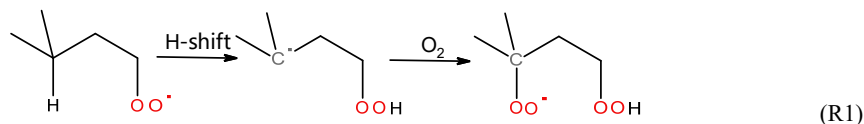
13 Highly oxygenated organic molecules (HOM) are found to play an important role in the formation and
14 growth of secondary organic aerosol (SOA). SOA is an important type of aerosol with significant impact on air
15 quality and climate. Compared with the oxidation of volatile organic compounds by O₃ and OH, HOM formation in
16 the oxidation by NO₃ radical, an important oxidant at night-time and dawn, has received less attention. In this study,
17 HOM formation in the reaction of isoprene with NO₃ was investigated in the SAPHIR chamber (Simulation of
18 Atmospheric PHotochemistry In a large Reaction chamber). A large number of HOM including monomers (C₃),
19 dimers (C₁₀), and trimers (C₁₅), both closed-shell compounds and open-shell peroxy radicals, were identified and
20 were classified into various series according to their formula. Their formation pathways were proposed based on the
21 peroxy radicals observed and known mechanisms in the literature, which were further constrained by the time profiles
22 of HOM after sequential isoprene addition to differentiate first- and second-generation products. HOM monomers
23 containing one to three N atoms (1-3N monomers) were formed, starting with NO₃ addition to carbon double bond,
24 forming peroxy radicals (RO₂), followed by autoxidation. 1N monomers were formed by both the direct reaction of
25 NO₃ with isoprene and of NO₃ with first-generation products. 2N-monomers (e.g. C₅H₈N₂O_n (n=8-13), C₅H₁₀N₂O_n (n=8-
26 14)) were likely the termination products of C₅H₉N₂O_n^{*}, which was formed by the addition of NO₃ to C₅-
27 hydroxynitrate (C₅H₉NO₄), a first-generation product containing one carbon double bond. 2N-monomers, which were
28 second-generation products, dominated in monomers and accounted for ~34% of all HOM, indicating the important
29 role of second-generation oxidation in HOM formation in isoprene+NO₃ under our reaction conditions. H-shift of
30 alkoxy radicals to form peroxy radicals and subsequent autoxidation (“alkoxy-peroxy” pathway) was found to be an
31 important pathway of HOM formation. HOM dimers were mostly formed by the accretion reaction of various HOM
32 monomer RO₂ and via the termination reactions of dimer RO₂ formed by further reaction of closed-shell dimers with
33 NO₃ and possibly by the reaction of C₅-RO₂ with isoprene. HOM trimers were likely formed by the accretion reaction
34 of dimer RO₂ with monomer RO₂. The concentrations of different HOM showed distinct time profiles during the
35 reaction, which was linked to their formation pathway. HOM concentrations either showed a typical time profile of
36 first-generation products, or of second-generation products, or a combination of both, indicating multiple formation
37 pathways and/or multiple isomers. Total HOM molar yield was estimated to be 1.2%^{+1.3%}_{-0.7%}, which corresponded to a
38 SOA yield of ~3.6% assuming the molecular weight of C₅H₉NO₆ as the lower limit. This yield suggests that HOM
39 may contribute a significant fraction to SOA yield in the reaction of isoprene with NO₃.



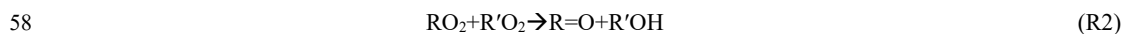
40 1 Introduction

41 Highly oxygenated organic molecules (HOM) are an important class of compounds formed in the oxidation
42 of volatile of organic compounds (VOC) including biogenic VOC and anthropogenic VOC (Crouse et al., 2013;
43 Ehn et al., 2014; Jokinen et al., 2014; Rissanen et al., 2014; Jokinen et al., 2015; Krechmer et al., 2015; Mentel
44 et al., 2015; Rissanen et al., 2015; Kenseth et al., 2018; Molteni et al., 2018; Garmash et al., 2019; McFiggans
45 et al., 2019; Molteni et al., 2019; Quelever et al., 2019). A number of recent studies have demonstrated that
46 HOM play a pivotal role in both nucleation and growth of secondary organic aerosol (SOA) (Ehn et al., 2014;
47 Kirkby et al., 2016; Tröstl et al., 2016). Particularly, in the early stage of aerosol growth, HOM may contribute
48 a significant fraction of SOA mass (Tröstl et al., 2016).

49 HOM are formed by the autoxidation of peroxy radicals (RO₂), which means they undergo intermolecular
50 H-shift forming alky radicals, followed by O₂ addition leading to formation of new RO₂ as shown in R1
51 (Vereecken et al., 2007; Crouse et al., 2013; Ehn et al., 2017; Bianchi et al., 2019; Moller et al., 2019;
52 Vereecken and Noziere, 2020).



54 Besides autoxidation, the RO₂ can also react with HO₂, RO₂ and NO₃, either forming a series of termination
55 products (R1-3), including organic hydroxyperoxide, alcohol, and carbonyl, or forming alkoxy radicals (RO,
56 R4-5) via the following reactions.



63 The termination products are detected in the mass spectra at masses M+1, M-15, M-17 respectively with
64 M being the molecular mass of the parent RO₂ (Ehn et al., 2014; Mentel et al., 2015). In case that RO₂ is an acyl
65 peroxy radical, percarboxylic acids and carboxylic acids are formed instead of hydroperoxides and alcohols in
66 R3 and R1, respectively (Atkinson et al., 2006; Mentel et al., 2015). RO₂ can also form HOM dimers by the
67 accretion reaction of two RO₂ (R6) (Berndt et al., 2018a; Berndt et al., 2018b; Valiev et al., 2019). Additionally,
68 HOM can be formed via H-shift in RO followed by O₂ addition (referred to as “alkoxy-proxy” pathway)
69 (Finlayson-Pitts and Pitts, 2000; Vereecken and Peeters, 2010; Vereecken and Francisco, 2012; Mentel et al.,
70 2015). These pathways are summarized in a recent comprehensive review (Bianchi et al., 2019), which also
71 further clarifies HOM definition.

72 Currently, most studies of HOM formation focus on the VOC oxidation by OH and O₃ (Crouse et al.,
73 2013; Ehn et al., 2014; Jokinen et al., 2014; Rissanen et al., 2014; Jokinen et al., 2015; Krechmer et al., 2015;



74 Mentel et al., 2015; Rissanen et al., 2015; Kenseth et al., 2018; Molteni et al., 2018; Garmash et al., 2019;
75 McFiggans et al., 2019; Molteni et al., 2019; Quelever et al., 2019). HOM formation in the oxidation of VOC
76 with NO_3 has received much less attention. NO_3 is another important oxidant of VOC mainly operating during
77 nighttime. Particularly, NO_3 has high reactivity with unsaturated BVOC such as monoterpene and isoprene. It
78 is often the dominant oxidant of these compounds at night, especially in regions where biogenic and
79 anthropogenic emissions mix (Geyer et al., 2001; Brown et al., 2009; Brown et al., 2011). The reaction products
80 contribute to SOA formation (Xu et al., 2015; Lee et al., 2016). Also, the organic nitrates produced in these
81 reactions play an important role in nitrogen chemistry by altering NO_x concentration, which further influences
82 photochemical recycling and ozone formation in the next day. Among these reaction products, HOM may also
83 be formed. Despite the potential importance, studies of HOM formation in the oxidation of BVOC by NO_3 are
84 still limited compared with the HOM formation via oxidation by O_3 and OH. Although a number of studies have
85 investigated the reaction of NO_3 with BVOC (Fry et al., 2009; Fry et al., 2011; Fry et al., 2014; Boyd et al.,
86 2015; Nah et al., 2016; Boyd et al., 2017; Clafin and Ziemann, 2018; Faxon et al., 2018; Draper et al., 2019;
87 Takeuchi and Ng, 2019), these studies mostly focus on either SOA yield and composition, or on the gas-phase
88 chemistry mechanism mainly for “traditional” oxidation products that stem from few oxidation steps.

89 Importantly, HOM formation in the reaction of NO_3 with isoprene, the most abundant BVOC accounting
90 for more than half of the global BVOC emissions, has not been explicitly addressed yet, to the best of our
91 knowledge. Although isoprene from plants are mainly emitted under light conditions, i.e., in the daytime, and
92 its chemical lifetime with respect to its reaction with OH is typically only a few hours, its concentration can
93 remain high after sunset. A substantial fraction of isoprene can then be oxidized by NO_3 (Brown et al., 2009).
94 Regarding the budget of NO_3 , the reaction of isoprene with NO_3 contributes to a significant fraction of NO_3 loss
95 at night, and in some circumstances even during the day, especially in the afternoon and afterwards (Ayres et
96 al., 2015). The reaction of isoprene with NO_3 is the subject of a number of studies (Ng et al., 2008; Perring et
97 al., 2009; Rollins et al., 2009; Kwan et al., 2012; Schwantes et al., 2015). These studies focus on the oxidation
98 mechanism and “traditional” oxidation products, as well as SOA yields. The initial step is the NO_3 addition to
99 one of the C=C double bonds, preferentially to the carbon C1 (Schwantes et al., 2015), followed by O_2 addition
100 forming a nitrooxyalkyl peroxy radical (RO_2). This RO_2 can undergo the reactions described above, forming a
101 series of products such as C5-nitrooxyhydroperoxide, C5-nitrooxycarbonyl, and C5-hydroxynitrate (Ng et al.,
102 2008; Kwan et al., 2012), as well as methyl vinyl ketone (MVK), potentially methacrolein (MACR),
103 formaldehyde, OH radical, and NO_2 as minor products (Schwantes et al., 2015). A high nitrate yield (57-95%)
104 was found (Perring et al., 2009; Rollins et al., 2009; Kwan et al., 2012; Schwantes et al., 2015). Products in the
105 particle phase such as C_{10} dimers were also detected (Ng et al., 2008; Kwan et al., 2012; Schwantes et al., 2015).
106 The SOA yield varies from 2% to 23.8% depending on the organic aerosol concentration (Ng et al., 2008;
107 Rollins et al., 2009). These studies have provided valuable insights in oxidation mechanism, particle yield and
108 composition. However, because HOM formation was not the focus of these studies, only a limited number of
109 products, mainly moderately oxygenated ones (oxygen number ≤ 2 in addition to NO_3 functional groups), were



110 detected in the gas phase. The detailed mechanism of HOM formation and their yields in the reaction of
111 BVOC+NO₃ are still unclear.

112 In this study, we investigated the HOM formation in the oxidation of isoprene by NO₃. We report the
113 identification of HOM, including HOM monomers, dimers, and trimers. According to the reaction products and
114 literature, we discuss the formation mechanism of these HOM. The formation mechanism of various HOM is
115 further constrained with time series of HOM upon repeated isoprene additions. We also provide an estimate of
116 HOM yield in isoprene+NO₃ and assess their roles in SOA formation.

117 2 Experimental

118 2.1 Chamber setup and experiments

119 Experiments investigating the reaction of isoprene with NO₃ were conducted in the SAPHIR chamber
120 (Simulation of Atmospheric PHotochemistry In a large Reaction chamber) at Forschungszentrum Jülich,
121 Germany. The details of the chamber have been described before (Rohrer et al., 2005; Zhao et al., 2015a; Zhao
122 et al., 2015b; Zhao et al., 2018). Briefly, SAPHIR is a Teflon chamber with a volume of 270 m³. It can utilize
123 natural sunlight for illumination and is equipped with a louvre system to switch between light and dark
124 conditions. In this study, the experiments were conducted in the dark with the louvres closed.

125 Temperature and relative humidity were continuously measured. Gas and particle phase species were
126 characterized using a comprehensive set of instruments with the details described before (Zhao et al., 2015b).
127 VOC were characterized using a Proton Transfer Reaction Time-of-Flight Mass Spectrometer (PTR-ToF-MS,
128 Ionicon Analytik, Austria). NO_x and O₃ concentrations were measured using a chemiluminescence NO_x analyzer
129 (ECO PHYSICS TR480) and an UV photometer O₃ analyzer (ANSYCO, model O341M), respectively. OH,
130 HO₂ and RO₂ concentrations were measured using a laser induced fluorescence system (LIF) (Fuchs et al., 2012).
131 NO₃ and N₂O₅ were detected by a custom-built instrument based on cavity ring-down spectroscopy. The design
132 of the instrument is similar to that described by Wagner et al. (2011). NO₃ was directly detected in one cavity
133 by its absorption at 662 nm and the sum of NO₃ and N₂O₅ in a second, heated cavity, which had a heated inlet
134 to thermally decompose N₂O₅ to NO₃. The sampling flow rate was 3 to 4 liters per minute. The detection by
135 cavity ring-down spectroscopy was achieved by a diode laser that was periodically switch on and off with a
136 repetition rate of 200 Hz. Ring-down events were observed by a digital oscilloscope PC card during the time
137 when the laser was switched off and were averaged over 1s. The zero-decay time that is needed to calculate the
138 concentration of NO₃ was measured every 20 s by chemically removing NO₃ in the reaction with excess nitric
139 oxide (NO) in the inlet system. The accuracy of measurements was limited by the uncertainty in the correction
140 for inlet losses of NO₃ and N₂O₅. In the case of N₂O₅ a transmission of (85±10) % was achieved and in the case
141 of NO₃ of (50±30) %.

142 Before an experiment, the chamber was flushed with high purity synthetic air (purity>99.9999% O₂ and N₂).
143 Experiments were conducted under dry condition. NO₂ and O₃ were added to the chamber first to form N₂O₅
144 and NO₃, reaching concentrations of ~60 ppb for NO₂ and ~100 ppb for O₃. After around half an hour, isoprene



145 was sequentially added into the chamber for three times at intervals of ~1 h. Around 40 min after the third
146 isoprene injection, NO₂ was added to compensate the loss of NO₃ and N₂O₅. Afterwards, three isoprene additions
147 were repeated in the same way as before. O₃ was added before the fifth and the sixth isoprene addition to
148 compensate for its loss by reaction. The schematic for the experimental procedure is shown in Fig. S1.
149 Experiments were designed such that the chemical system was dominated by the reaction of isoprene with NO₃
150 and the reaction of isoprene with O₃ did not play a major role. Figure S2 shows the relative contributions of the
151 reaction of O₃ and NO₃ with isoprene to the total chemical loss of isoprene using the NO₃ and O₃ concentrations
152 measured. The reaction with NO₃ accounted for >95% of the isoprene consumption at all time.

153 2.2 Characterization of HOM

154 HOM were detected using a Chemical Ionization time-of-flight Mass Spectrometer (Aerodyne Research Inc.,
155 USA) with nitrate as the reagent ion (CIMS). ¹⁵N nitric acid was used to produce ¹⁵NO₃⁻ in order to distinguish
156 the NO₃ group in target molecules formed in the reaction from the reagent ion. The details of the instrument are
157 described in our previous publications (Ehn et al., 2014; Mentel et al., 2015; Pullinen et al., 2020). The CIMS
158 has a mass resolution of ~4000 (m/dm). HOM concentrations were estimated using the calibration coefficient
159 of H₂SO₄ as described by Pullinen et al. (2020) because the charge efficiency of HOM and H₂SO₄ can be
160 assumed to be equal and close to the collision limit (Ehn et al., 2014; Pullinen et al., 2020). The details of the
161 calibration with H₂SO₄ are provided in the supplement S1. The HOM yield was derived using the concentration
162 of the HOM produced, divided by the concentration of isoprene that was consumed by NO₃. The loss of HOM
163 to the chamber was corrected using a wall loss rate of 6×10⁻⁴ s⁻¹ as quantified previously (Zhao et al., 2018).
164 HOM concentrations were also corrected for dilution due to the replenishment flow needed to maintain a
165 constant overpressure of the chamber (loss rate ~1×10⁻⁶ s⁻¹) (Zhao et al., 2015b). The influence of wall loss
166 correction and dilution correction on HOM yield was ~12% and <1%, respectively.

167 3 Results and discussion

168 3.1 Overview of HOM

169 The mass spectra of HOM in the gas phase formed in the oxidation of isoprene by NO₃ are shown in
170 Fig. 1. A large number of HOM were detected. The reaction products can be roughly divided into three classes:
171 monomers (C₅, ~200-400 Th), dimers (C₁₀, ~400-600 Th), and trimers (C₁₅, ~>600 Th), according to their
172 mass to charge ratio (m/z). The detailed peak assignment of monomers, dimers, and trimers is discussed in the
173 following sections.

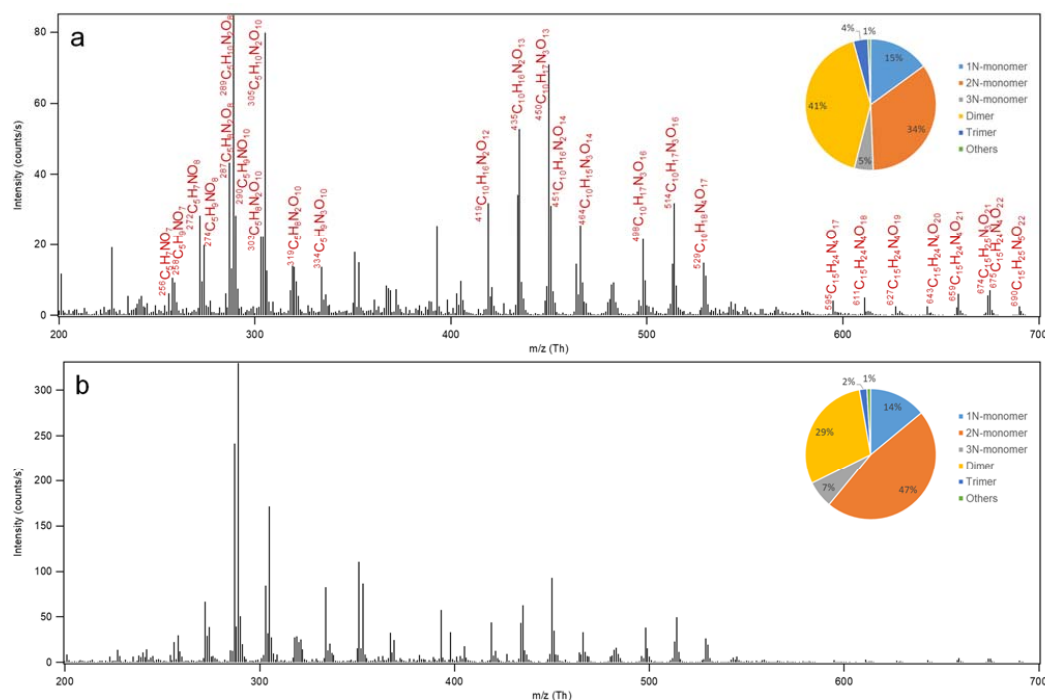
174 3.2 HOM monomers and their formation

175 3.2.1 Overview of HOM monomers

176 HOM monomers showed a roughly repeating pattern in the mass spectrum at every 16 Th
177 (corresponding to the mass of oxygen) (Fig. 1a). Here a number of series of HOM monomers with continuously



178 increasing oxygenation were found, such as $C_5H_9NO_8$, $C_5H_7NO_8$, $C_5H_8N_2O_8$, $C_5H_{10}N_2O_8$ (Table 1, Table S1-2
179 and Fig. 2). These monomers included both stable closed-shell molecules and open-shell radicals, such as
180 $C_5H_8NO_n\cdot$ and $C_5H_9N_2O_n\cdot$. The open-shell molecules were likely RO_2 radicals because of their much longer life
181 time and hence higher concentrations compared with alkoxy radicals (RO) and alkyl radicals (R). Since the
182 observed stable products were mostly termination products of RO_2 reactions, we describe the stable products in
183 a RO_2 -oriented approach. It is worth noting that some of the termination products may contain multiple isomers
184 formed from different pathways.

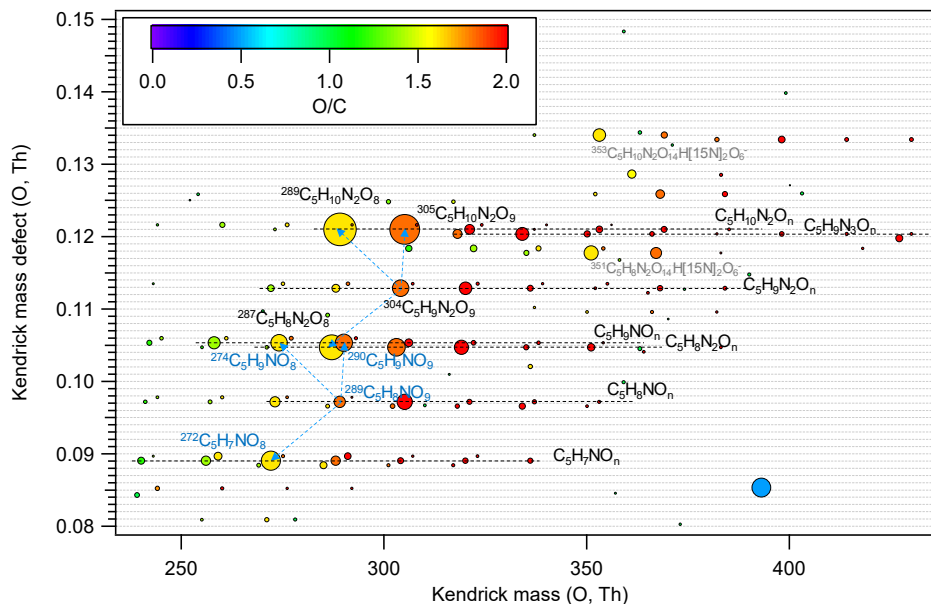


185
186 Figure 1. Mass spectrum of the HOM formed in the oxidation of isoprene by NO_3 . Panel a and b show
187 the average spectrum during the first isoprene addition period (P1) and for the whole period of six isoprene
188 additions (P1-6), respectively. The insets show the contributions of different classes of HOM. 1-3N-monomer
189 refers to the monomers containing 1-3 nitrogen atoms in the molecular formula.

190 HOM monomers were classified into 1N-, 2N-, and 3N-monomers according to the number of nitrogen
191 atoms that they contain. The contribution of 2N-monomers such as $C_5H_{10}N_2O_8$ and $C_5H_8N_2O_8$ was higher than that
192 of the 1N-HOM monomers, and that of 3N-monomers was the least (Fig. 1, inset). The most abundant monomers
193 were $C_5H_{10}N_2O_8$, $C_5H_{10}N_2O_9$, and $C_5H_8N_2O_8$. The termination products of $C_5H_9NO_8$, $C_5H_9NO_9$, and $C_5H_7NO_8$ also
194 showed relatively high abundance. These limited number of compounds dominated the HOM monomers. Since 2N-
195 monomers were second-generation products as discussed below, the higher abundance 2N- monomers indicate that
196 the second-generation HOM play an important role in the reaction of NO_3 with isoprene in the reaction conditions of
197 our study, as also seen by Wu et al. (2020). This is more evident for the mass spectrum averaged over six isoprene



198 addition periods (Fig. 1b), where the abundance of $C_5H_{10}N_2O_n$ and $C_5H_8N_2O_n$ were more dominant. This observation
 199 is in contrast with the finding for the reaction of O_3 with BVOC which contains only one double bond such as α -
 200 pinene (Ehn et al., 2014), where HOM are mainly first-generation products formed via autoxidation.



201
 202 Figure 2. Kendrick mass defect plot for O of HOM monomers. The size (area) of circles is set to be proportional to the
 203 average peak intensity of each molecular formula during the first isoprene addition period (P1). The species at m/z 351 and
 204 353 (labelled in grey) are the adducts of $C_5H_8N_2O_8$ and $C_5H_8N_2O_8$ with $H[15N]_2O_6$, respectively. The blue dashed lines
 205 with arrows indicate the termination product hydroperoxide (M+H), alcohol (M-O+H), and ketone (M-O-H) with M the
 206 molecular formula of a HOM RO_2 .

207 3.2.2 1N-monomers

208 In our experiments we observed a $C_5H_8NO_n$ ($n=7-12$) series (series M1), as well as its corresponding
 209 termination products $C_5H_7NO_{n-1}$, $C_5H_9NO_{n-1}$, and $C_5H_9NO_n$ via the reactions with RO_2 and HO_2 , which contain
 210 carbonyl, hydroxyl, and hydroperoxy group, respectively. Overall, the peak intensities of $C_5H_9NO_n$ and
 211 $C_5H_7NO_n$ series first increased and then decreased as oxygen number increased (Fig. 2), with the peak intensity
 212 of $C_5H_9NO_8$ and $C_5H_7NO_8$ being the highest within their respective series when averaged over the whole
 213 experiment period.

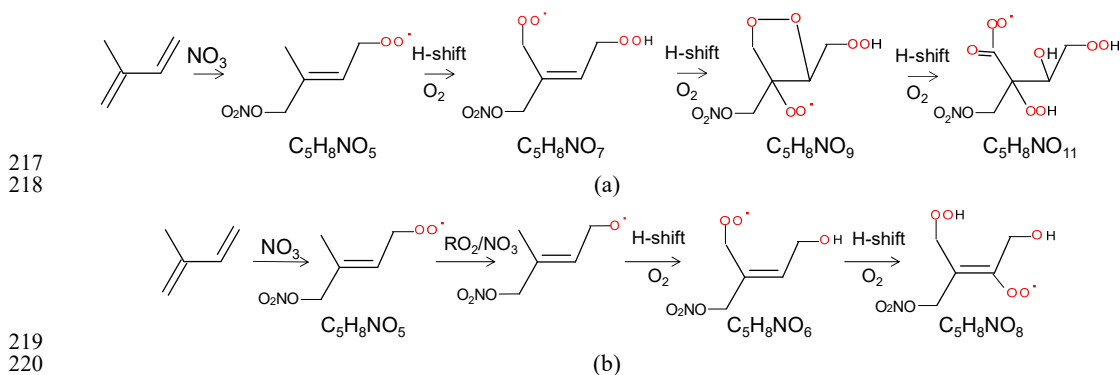
214 Table 1. HOM monomers formed in the oxidation of isoprene by NO_3 .

Series Number	Product	Type ^a	Pathway of RO_2
M1a/b	$C_5H_8NO_n$ ($n=7-12$)	RO_2	
	$C_5H_9NO_n$	ROOH	Isoprene+ NO_3
	$C_5H_9NO_{n-1}$	ROH	Isoprene+ NO_3 + NO_3
	$C_5H_7NO_{n-1}$	R=O	



M2a/b	$C_5H_9N_2O_n$ ($n=9-14$)	RO_2	Isoprene + NO_3 + NO_3
	$C_5H_{10}N_2O_n$	ROOH	
	$C_5H_{10}N_2O_{n-1}$	ROH	
	$C_5H_8N_2O_{n-1}$	R=O	
	$C_5H_9N_3O_{n+2}$	PN	
M3	$C_5H_7N_2O_n$ ($n=9$)	RO_2	Isoprene + NO_3 + NO_3
	$C_5H_8N_2O_n$	ROOH	
	$C_5H_8N_2O_{n-1}$	ROH	
	$C_5H_6N_2O_{n-1}$	R=O	
M4	$C_5H_{10}NO_n$ ($n=8-9$)	RO_2	Isoprene + NO_3 + OH
	$C_5H_{11}NO_n$	ROOH	
	$C_5H_{11}NO_{n-1}$	ROH	
	$C_5H_9NO_{n-1}$	R=O	

215 ^a: RO_2 denotes peroxy radical and ROOH, ROH, and R=O denote the termination products containing
 216 hydroperoxy, hydroxyl, and carbonyl group, respectively.



221 Scheme 1. The pathway to form HOM RO_2 $C_5H_8NO_n\bullet$ ($n=7, 9, 11$) series (a) and $C_5H_8NO_n\bullet$ ($n=8, 10,$
 222 12) series (b) in the reaction of isoprene with NO_3 .

223 $C_5H_8NO_n\bullet$ with odd number oxygen atoms ($n=7, 9, 11$, series M1a) were possibly formed by the attack
 224 of NO_3 to one double bond (preferentially to C1 according to previous studies (Skov et al., 1992; Berndt and
 225 Böge, 1997; Schwantes et al., 2015) and followed by autoxidation (Scheme 1a). We would like to note that
 226 NO_3^- -CIMS only observed HOM with oxygen numbers ≥ 6 in this study due to its selectivity of detection.
 227 $C_5H_8NO_n\bullet$ with even number oxygen atoms ($n=8, 10, 12$) (series M1b in Table 1) were possibly formed after
 228 H-shift of an alkoxy radical formed in reaction R5 or R6 and subsequent O_2 addition (“alkoxy-peroxy” channel)
 229 (Scheme 1b). The RO_2 can undergo further autoxidation adding two oxygen atoms after each H-shift.

230 Some HOM monomers may contain multiple isomers and be formed via different pathways. For example,
 231 $C_5H_9NO_n$ can contain alcohols ($C_5H_9NO_n$) corresponding to RO_2 $C_5H_8NO_{n+1}\bullet$, hydroperoxides ($C_5H_9NO_n$)
 232 corresponding to RO_2 $C_5H_8NO_n\bullet$ or the ketones from RO_2 $C_5H_{10}NO_{n+1}\bullet$. Some RO_2 $C_5H_8NO_n\bullet$ may be formed via
 233 the reaction of first-generation products with NO_3 in addition to direct reaction of isoprene with NO_3 . For example,
 234 $C_5H_8NO_7\bullet$ can be formed by the reaction of NO_3 with $C_5H_8O_2$, which is a first-generation product observed previously



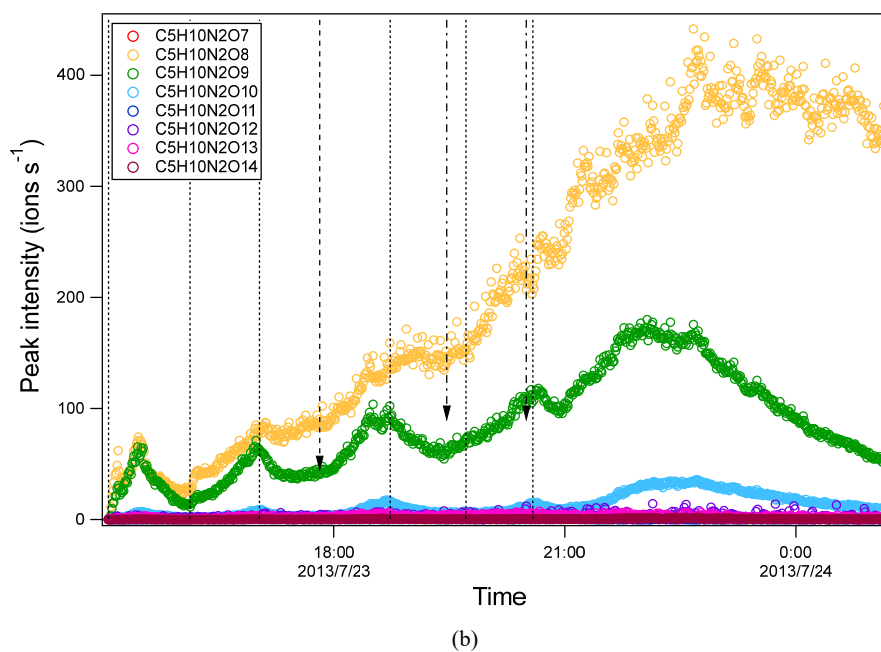
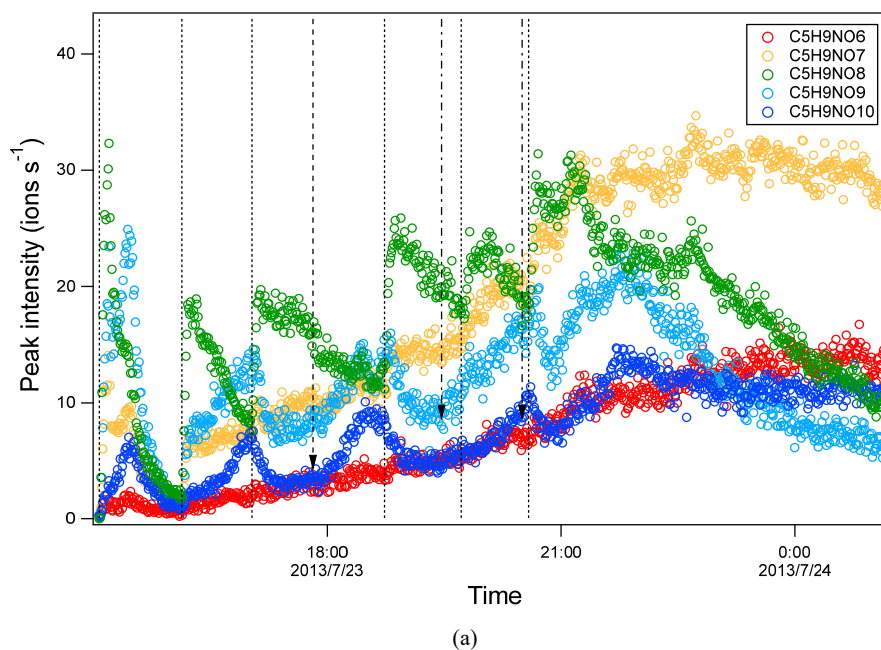
235 in in the reaction of isoprene with NO_3 or OH (Scheme S1b) (Kwan et al., 2012). Moreover, $\text{RO}_2 \text{C}_5\text{H}_8\text{NO}_n\bullet$ can be
236 formed from C5-carbonylnitrate, a first-generation product, with OH (Scheme S1a). Trace amount of OH can be
237 produced in the reaction isoprene with NO_3 (Kwan et al., 2012; Wennberg et al., 2018). OH can also be formed via
238 Criegee intermediates formed in isoprene+ O_3 (Nguyen et al., 2016), but this OH source was likely minor because the
239 contribution of isoprene+ O_3 to total isoprene loss was negligible (<5%, Fig. S2). $\text{C}_5\text{H}_8\text{NO}_8\bullet$ may also be formed by
240 the reaction of NO_3 with $\text{C}_5\text{H}_8\text{O}_3$, which is a first-generation product observed in the reaction of isoprene with OH
241 (Kwan et al., 2012). The $\text{C}_5\text{H}_8\text{NO}_n\bullet$ formed via direct reaction of isoprene with NO_3 is a first-generation RO_2 while
242 that formed via other indirect pathways is a second-generation RO_2 . The time profile of the isomers from these two
243 pathways, however, are expected to be different as will be discussed below.

244 Time series of HOM can shed light on their formation mechanisms. It is expected that first-generation
245 products increase fast with isoprene addition and reach a maximum earlier in the presence of wall loss of organic
246 vapour, while second-generation products reach a maximum in the later stage or increase continuously if the
247 production rate is higher than the loss rate. As a reference to analyze the time profiles of HOM, the times profile of
248 isoprene, NO_3 , and N_2O_5 are also shown (Fig. S3). After isoprene was added in each period, NO_3 and N_2O_5 dropped
249 dramatically and then gradually increased. We found that termination products within the same M1 series showed
250 different time profiles. For example, in $\text{C}_5\text{H}_9\text{NO}_n$ series, $\text{C}_5\text{H}_9\text{NO}_8$ clearly increased instantaneously with isoprene
251 addition, and decreased fast afterwards (Fig. 3a), indicating that it was a first-generation product, which was expected
252 according to the mechanism Scheme 1. $\text{C}_5\text{H}_9\text{NO}_6$ and $\text{C}_5\text{H}_9\text{NO}_{10}$ had a general increasing trend with time. While
253 $\text{C}_5\text{H}_9\text{NO}_6$ increased continuously with time, $\text{C}_5\text{H}_9\text{NO}_{10}$ reached maximum intensity in the late phase of each isoprene
254 addition period and then decreased naturally or after isoprene addition. The faster loss of $\text{C}_5\text{H}_9\text{NO}_{10}$ may result from
255 the faster wall loss due to its lower volatility. $\text{C}_5\text{H}_9\text{NO}_7$ and $\text{C}_5\text{H}_9\text{NO}_9$ showed a mixing time profile with features of
256 the former two kinds of time profiles, increasing almost instantaneously with isoprene additions especially in the first
257 two periods while increasing continuously or decreasing first with isoprene additions and then increasing later in
258 each periods. This kind of time series indicates that there were significant contributions from both first- and second-
259 generation products.

260 The second-generation products may be different isomers formed in pathways other than Scheme 1. Second-
261 generation $\text{C}_5\text{H}_9\text{NO}_6$ can be formed via $\text{C}_5\text{H}_8\text{NO}_7\bullet$, which can also be formed by the reaction of NO_3 and O_2 with
262 $\text{C}_5\text{H}_8\text{O}_2$ as mentioned above (Scheme S2b), or by the reaction of OH with $\text{C}_5\text{H}_7\text{NO}_4$ (Scheme S2a). The time series
263 of $\text{C}_5\text{H}_8\text{NO}_7\bullet$ did show the contribution of both the first- and second-generation processes, which generally
264 increased with time while also responding to isoprene addition (Fig. S4). The time profiles of $\text{C}_5\text{H}_8\text{NO}_8\bullet$ showed
265 more contribution of second-generation processes because it continuously increased with time in general. If the
266 pathways via the reaction of NO_3 and O_2 with $\text{C}_5\text{H}_8\text{O}_2$ and the reaction of OH with $\text{C}_5\text{H}_7\text{NO}_4$ contribute most to
267 $\text{C}_5\text{H}_9\text{NO}_6$, $\text{C}_5\text{H}_9\text{NO}_6$ would show mostly a time profile of second-generation products. For the RO_2 in $\text{C}_5\text{H}_8\text{NO}_n\bullet$
268 series, the peak of $\text{C}_5\text{H}_8\text{NO}_n\bullet$ overlaps with $\text{C}_5\text{H}_{10}\text{N}_2\text{O}_n$ in the mass spectra, which is a much larger peak, and thus
269 cannot be differentiated from $\text{C}_5\text{H}_{10}\text{N}_2\text{O}_n$. Therefore, it is not possible to obtain reliable separate time profiles in
270 order to differentiate their major sources. It is worth noting that nitrate CIMS may not be able to sensitively detect
271 all isomers of $\text{C}_5\text{H}_9\text{NO}_6$ due to the sensitivity limitation. Therefore, we cannot exclude the possibility that the



272 absence of some first-generation isomers of $C_5H_9NO_6$ was due to the low sensitivity of these isomers. Similar to
273 $C_5H_9NO_6$, the second-generation pathway for $C_5H_9NO_7$, $C_5H_9NO_9$, and $C_5H_9NO_{10}$ are shown in Scheme S1, S3, S4.



278 Figure 3. Time series of peak intensity of several HOM monomers of $C_5H_9NO_n$ series (a) and of $C_5H_{10}N_2O_n$
279 series (b). They are likely the termination products of $RO_2 C_5H_8NO_n^\bullet$ and $C_5H_9N_2O_n^\bullet$, respectively. The dashed lines



280 indicate the time of isoprene additions. The long-dashed arrow indicates the time of NO₂ addition. The dash-dotted
281 arrows indicate the time of O₃ additions.

282 Among the termination products of the 1N-monomer RO₂, carbonyl and hydroxyl/hydroperoxide
283 species had comparable abundance in general (Table S1), suggesting that disproportionation reactions between
284 RO₂ and RO₂ forming hydroxy and carbonyl species (R1-2) was likely an important RO₂ termination pathway.
285 However, dependence of the exact ratio of carbonyl species to hydroxyl/hydroperoxide species on the number
286 of oxygen atoms did not show a clear trend (Table S1), suggesting that the reactions of HOM RO₂ depended on
287 their specific structure. There was no clear difference in the abundance between the termination products from
288 C₅H₈NO_n• with odd and even number of oxygen atom in general, although the most abundant termination
289 product of C₅H₈NO_n•, i.e. C₅H₇NO₈, was likely formed from C₅H₈NO₉• in series M1a. This fact indicates that
290 both the peroxy pathway and alkoxy-peroxy pathway were important for the HOM formation in isoprene+NO₃
291 under our conditions.

292 In addition to the termination products of RO₂ M1, minor peaks of the RO₂ series C₅H₁₀NO_n• (n=8-9) (M4,
293 Table 1) and their corresponding termination products including hydroperoxide, alcohol and carbonyl species were
294 detected (Table S3). C₅H₁₀NO_n were likely formed by sequential addition of NO₃ and OH to two double bonds of
295 isoprene (Scheme S5). OH can react fast with isoprene or with the first-generation products of the reaction of isoprene
296 with NO₃, thus forming C₅H₁₀NO_n•. In addition, a few very minor but noticeable peaks of C₅H₉O_n• and their
297 corresponding termination products C₅H₁₀O_n and C₅H₈O_n were also observed. These HOM may be formed by the
298 reactions of isoprene with trace amount of OH and with O₃, although their contributions to reacted isoprene were
299 negligible. These HOM were also observed in the reaction of isoprene with O₃ with and without OH scavengers
300 (Jokinen et al., 2015).

301 Among 1N-monomer HOM, C₅H₉NO₇ has been observed in the particle phase using ESI-TOFMS by
302 Ng et al. (2008) while others have not been observed in previous laboratory studies of the reaction of isoprene
303 with NO₃, to our knowledge. A number of C₅ organic nitrates have been observed in field studies. For example,
304 C₅H₇₋₁₁NO₄₋₉ have been observed in aerosol particles during the Southern Oxidant and Aerosol Study in rural
305 Alabama, US, where isoprene is abundant. Those compounds were also observed in chamber experiments of
306 the reaction of isoprene with OH in the presence of NO_x (Lee et al., 2016).

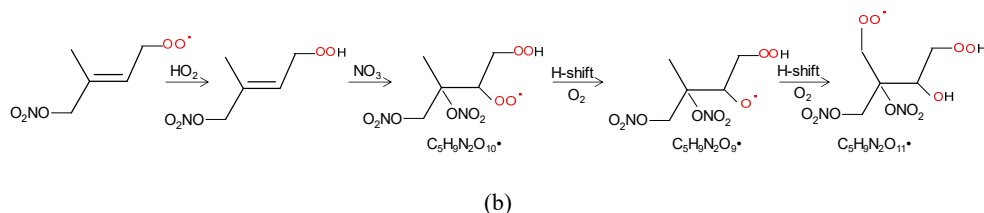
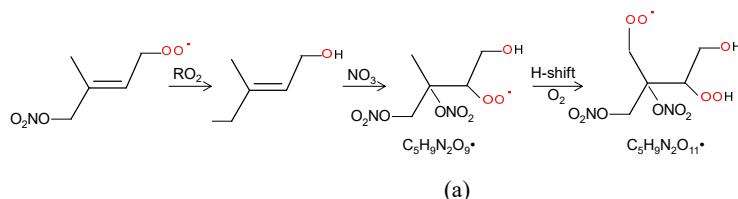
307 3.2.3 2N-monomers

308 2N-monomer RO₂, C₅H₉N₂O_n•(n=9-14) series, were observed, as well as its likely termination products,
309 C₅H₈N₂O_n and C₅H₁₀N₂O_n, which contain a carbonyl and hydroxyl or hydroperoxide functional group,
310 respectively. The RO₂ series C₅H₉N₂O_n• with even number of oxygen atoms (n=9, 11) (M2a in Table 1) were
311 likely formed from the first-generation product C₅H₉NO₄ (C5-hydroxynitrate) by adding NO₃ to the remaining
312 double bond, forming C₅H₉N₂O₉•, followed by autoxidation (Scheme 2a). This RO₂ series can also be formed
313 by the addition of NO₃ to the double bond of first-generation products (e.g. C₅H₉NO₅, C5-
314 nitroxyhydroperoxide) and subsequent alkoxy-peroxy step (Scheme 2b). C₅H₉N₂O_n• with even number of
315 oxygen atoms (n=8, 10, 12) (M2b in Table 1), can be formed by the addition of NO₃ to the double bond of

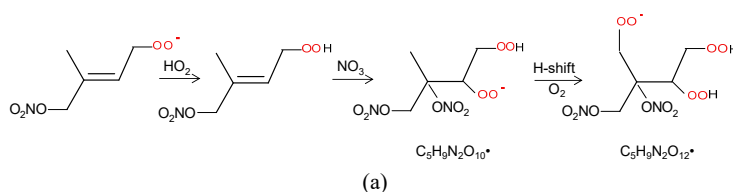


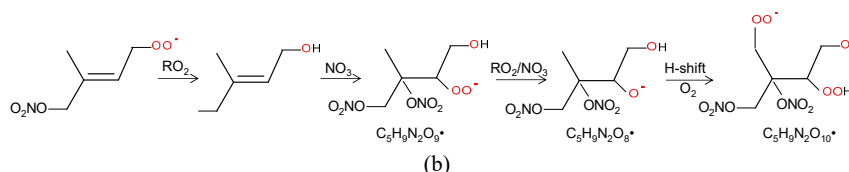
316 C₅H₉NO₅ followed by autoxidation (Scheme. 3a), or of C₅H₉NO₄ followed by alkoxy-peroxy step (Scheme. 3b).
 317 The formation pathways of C₅H₉N₂O_{13/14}• cannot be well explained, as they contain too many oxygen atoms to
 318 be formed via the pathways in Scheme 2 or 3.

319 Formation through either Scheme 2 or 3 means that C₅H₈N₂O_n and C₅H₁₀N₂O_n were second-generation
 320 products. The time series of C₅H₁₀N₂O_n species clearly indicates that they were indeed second-generation
 321 products. C₅H₁₀N₂O_n species generally did not increase immediately with isoprene addition (Fig. 3b), but
 322 increased gradually with time and reached its maximum in the later stage of each period before decreasing with
 323 time (in the period 1 and 6), or decreasing after the next isoprene addition (periods 2-5). This time profile can
 324 be explained by the time series of the precursor of C₅H₁₀N₂O_n, C₅H₉N₂O_n• (RO₂) (Fig. S5). The changing rate
 325 (production rate minus destruction rate) of C₅H₁₀N₂O_n concentration was dictated by the concentration of
 326 C₅H₉N₂O_n• and the wall loss rate. During periods 2 to 5, C₅H₉N₂O_n• gradually increased but decreased sharply
 327 after the isoprene additions, resulted from chemical reactions of C₅H₉N₂O_n• and additionally from wall loss.
 328 When the rate of change of the C₅H₁₀N₂O_n concentration was positive, the concentration of C₅H₁₀N₂O_n increased
 329 with time. After isoprene additions, the rate of change of the C₅H₁₀N₂O_n concentration decreased dramatically
 330 to even negative, leading to decreasing concentrations. Similar to C₅H₁₀N₂O_n, the C₅H₈N₂O_n series did not
 331 respond immediately to isoprene additions (Fig. S6), which is expected for second-generation products
 332 according to the mechanism discussed above (Scheme 2-3). Particularly, the continuing increase of C₅H₈N₂O_n
 333 after isoprene was completely depleted (~ at 21:40, Fig. S6) clearly indicates that these compounds were second-
 334 generation products, although in the end they decreased due to wall loss.



339 Scheme 2. The pathway to form C₅H₉N₂O_n (n=9, 11) HOM RO₂ series by RO₂ channel (a) and alkoxy-
 340 peroxy channel.





343
344
345
346

Scheme 3. The pathway to form $C_5H_9N_2O_n$ ($n=8, 10, 12$) HOM RO_2 series by RO_2 channel (a) and alkoxy-peroxy channel (b).

347 According to the finding of Ng et al. (2008), C5-hydroxynitrate decays much faster than C5-
348 nitrooxyhydroperoxides. Therefore, it is likely that $C_5H_9N_2O_n$ • M2a series was mainly formed from $C_5H_9NO_4$
349 instead of $C_5H_9NO_5$, while $C_5H_9N_2O_n$ • M2b were formed from $C_5H_9NO_4$ followed by an alkoxy-peroxy step.
350 That is, Scheme 2 was more likely.

351 Similar to $C_5H_8NO_n$ •, the intensity of carbonyl species from $C_5H_9N_2O_n$ • was also comparable with that
352 of hydroxyl/hydroperoxide species, suggesting that RO_2+RO_2 reaction forming ketone and alcohol was likely
353 an important pathway of HOM formation in isoprene+ NO_3 . In general, the intensity of the termination products
354 from $C_5H_9N_2O_n$ • with both even and odd oxygen numbers were comparable. This again suggests that both
355 peroxy and alkoxy-peroxy pathways were important for HOM formation in isoprene+ NO_3 . The intensity of
356 $C_5H_{10}N_2O_n$ and $C_5H_8N_2O_n$ decreased with oxygen number with the $C_5H_{10}N_2O_8$ and $C_5H_8N_2O_8$ being the most
357 abundant within their respective series.

358 Some 2N-monomers have been detected in previous studies of the reaction of isoprene with NO_3 .
359 $C_5H_{10}N_2O_8$ has been detected in the particle phase by Ng et al. (2008) and $C_5H_8N_2O_7$ was detected in the gas
360 phase by Kwan et al. (2012). $C_5H_9N_2O_9$ • has been proposed to be formed via the pathway as in Scheme 2a (Ng
361 et al., 2008), and it was directly detected in our study. $C_5H_8N_2O_7$ species has been proposed to be a dinitrooxy
362 epoxide formed by the oxidation of nitrooxyhydroperoxide (Kwan et al., 2012), instead of being a dinitrooxy
363 ketone proposed in our study, a termination product of $C_5H_9N_2O_8$ •. Admittedly, $C_5H_8N_2O_7$ may contain both
364 isomers. In addition, Ng et al. (2008) detected $C_5H_8N_2O_6$ in the gas phase, which was not detected in this study
365 likely due to the selectivity of NO_3 -CIMS.

366 One could suppose that $C_5H_7N_2O_n$ • should also be formed since C5-nitrooxycarbonyl ($C_5H_7NO_4$) also
367 contains one double bond that can be attacked by NO_3 in a second oxidation step. However, concentrations of
368 $C_5H_7N_2O_n$ were too low to assign molecular formulas with confidence except for $C_5H_7N_2O_9$ •, clearly showing
369 that $C_5H_7N_2O_n$ • was not important. This fact is consistent with the finding of Ng et al. (2008) that C5-
370 nitrooxycarbonyls react slowly with NO_3 . In addition, the presence of HOM containing two N atoms is in line
371 with the finding by Faxon et al. (2018) who detected products containing two N atoms in the reaction of NO_3
372 with limonene, which also contain two carbon double bonds. It is anticipated that for VOCs with more than one
373 double bond, NO_3 can add to all the double bonds as for isoprene and limonene.



374 **3.2.4 3N-monomers**

375 HOM containing three nitrogen atoms, $C_5H_9N_3O_n$ ($n=9-16$), were observed. These compounds were
376 possibly peroxy nitrates formed by the reaction of RO_2 ($C_5H_9N_2O_{n-2}\bullet$) with NO_2 . The time series of $C_5H_9N_3O_n$
377 was examined to check whether they match such a mechanism. If $C_5H_9N_3O_n$ were formed by the reaction of
378 $C_5H_9N_2O_{n-2}\bullet$ with NO_2 , the concentration would be a function of the concentrations of $C_5H_9N_2O_{n-2}\bullet$ and NO_2 as
379 follows:

$$380 \quad \frac{d[C_5H_9N_3O_n]}{dt} = k[C_5H_9N_2O_{n-2}\bullet][NO_2] - k_{wl}[C_5H_9N_3O_n]$$

381 where $[C_5H_9N_3O_n]$, $[C_5H_9N_2O_{n-2}\bullet]$, and $[NO_2]$ are the concentration of these species, k is the rate
382 constant and k_{wl} is the wall loss rate. Because the products of $C_5H_9N_2O_{n-2}\bullet$ and NO_2 were at their maximum at
383 the end of each period and decreased rapidly after isoprene addition (Fig. S7), the concentration should have
384 the maximum increasing rate at the end of each isoprene addition period. However, we found that only
385 $C_5H_9N_3O_{12,15,16}$ showed such a time profile (Fig. S8), while $C_5H_9N_3O_{9,10,11,13,14}$ generally increased with time,
386 different from what one would expect based on the proposed pathway. Therefore, it is likely that $C_5H_9N_3O_{12,15,16}$
387 were mainly formed via the reaction of $C_5H_9N_2O_n\bullet$ with NO_2 , whereas $C_5H_9N_3O_{9,10,11,13,14}$ were not. Moreover,
388 $C_5H_9N_3O_9$ cannot be explained by the reaction $C_5H_9N_2O_n\bullet$ ($n \geq 9$) with NO_2 or NO_3 , because these reactions
389 would add at least one more oxygen atom. One possible pathway to form $C_5H_9N_3O_9$ was the direct addition of
390 N_2O_5 to the carbon double bond of C5-hydroxynitrate, forming a nitronitrate. Such a mechanism has been
391 proposed previously in the heterogeneous reaction of N_2O_5 with 1-palmitoyl-2-oleoyl-sn-glycero-3-
392 phosphocholine (POPC) because $-NO_2$ and $-NO_3$ groups were detected (Lai and Finlayson-Pitts, 1991). This
393 pathway generally matched the time series of $C_5H_9N_3O_{9,10,11,13,14}$ typical of second-generation products since
394 C5-hydroxynitrate was a first-generation product. It is possible that the main pathway of $C_5H_9N_3O_{9,10,11,13,14}$ was
395 the reaction of $C_5H_9NO_{4,5,6}$ with N_2O_5 , although the reaction of N_2O_5 with C=C double bonds in common alkenes
396 and unsaturated alcohols are believed to be not important (Japar and Niki, 1975; Pfrang et al., 2006).

397 3N-monomers, $C_5H_9N_3O_{10}$, has been observed in the particles formed in isoprene+ NO_3 by Ng et al.
398 (2008). Here a complete series of $C_5H_9N_3O_n$ were observed. $C_5H_9N_3O_{10}$ was previously proposed to be formed
399 by another pathway, i.e. the reaction of RO_2 ($C_5H_9N_2O_9\bullet$) and NO_3 (Ng et al., 2008). We further examined the
400 possibility of such a pathway in our study. Similar to NO_2 , if $C_5H_9N_3O_n$ were formed by the reaction of
401 $C_5H_9N_2O_{n-2}\bullet$ with NO_3 , the concentration would have the maximum increasing rate at the end of each isoprene
402 addition period. Among $C_5H_9N_2O_n\bullet$, the precursors of $C_5H_9N_3O_n$, $C_5H_9N_2O_{9,10,13,14}\bullet$ showed a maximum
403 increasing rate and a subsequent decrease after isoprene addition. The difference in oxygen number between
404 $C_5H_9N_3O_{12,15,16}$, the termination products, and $C_5H_9N_2O_{9,10,13,14}\bullet$, the corresponding RO_2 with the consistent
405 time profile is mostly two. Since the reaction of $C_5H_9N_2O_n$ with NO_2 and NO_3 result an increased oxygen number
406 by two and by one, respectively, we infer that it is more likely that $C_5H_9N_3O_{12,15,16}$ were formed by the reaction
407 of $C_5H_9N_2O_{10,13,14}\bullet$ with NO_2 rather than NO_3 , and thus they were likely peroxy nitrates rather than nitrates



408 formed by the reaction of RO₂ with NO₃. Since alkyl peroxy nitrates decompose rapidly (Finlayson-Pitts and
409 Pitts, 2000; Ziemann and Atkinson, 2012), it is possible that these compounds contained peroxyacetyl nitrates.

410 Little attention has been paid to the RO₂+NO₂ pathway in nighttime chemistry of isoprene in the
411 literature (Wennberg et al., 2018), which is likely due to the stability of the products. According to this pathway,
412 C₅H₈N₂O_n, which was proposed to be a ketone formed via C₅H₉N₂O₉• in the M2 series (Table 1) as discussed
413 above, can also comprise peroxy nitrates formed by the reaction of C₅H₈NO_n• (M1a RO₂) with NO₂.

414 3.3 HOM dimers and their formation

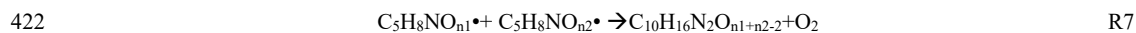
415 Table 2. HOM dimers and trimers formed in the oxidation of isoprene by NO₃.

Series Number	Formula	Type	Pathway of RO ₂
Dimer 1	C ₁₀ H ₁₆ N ₂ O _n (n=10-17)	ROOR ^a	M1 ^b +M1
Dimer 2	C ₁₀ H ₁₇ N ₃ O _n (n=11-19)	ROOR	M1+M2/M3+M4
Dimer 3	C ₁₀ H ₁₈ N ₄ O _n (n=15-18)	ROOR	M2+M2
Dimer 4	C ₁₀ H ₁₈ N ₂ O _n (n=10-16)	ROOR	M1+M4
Dimer 5	C ₁₀ H ₁₅ N ₃ O _n (n=13-17)	ROOR	M1+M3
Dimer 6	C ₁₀ H ₁₉ N ₃ O _n (n=14-15)	ROOR	M2+M4
Dimer 7	C ₁₀ H ₁₄ N ₂ O _n (n=11-12)	ROOR	Unknown
Dimer 8	C ₁₀ H ₁₅ NO _n (n=9-12)	ROOR	C ₁₀ H ₁₆ NO _n
Dimer 9	C ₁₀ H ₁₇ NO _n (n=11-19)	ROOR	C ₁₀ H ₁₆ NO _n
Dimer R1	C ₁₀ H ₁₆ N ₃ O _n (n=12-15)	RO ₂	Dimer 1+NO ₃
Dimer R2	C ₁₀ H ₁₇ N ₂ O _n (n=11-12)	RO ₂	Dimer 1+OH
Dimer R3	C ₁₀ H ₁₇ N ₄ O _n (n=16-18)	RO ₂	Dimer 2+NO ₃
Dimer R4	C ₁₀ H ₁₆ NO _n (n=10-16)	RO ₂	M1+C ₅ H ₈
Trimer 1	C ₁₅ H ₂₄ N ₄ O _n (n=17-23)	ROOR	Dimer R1+M1
Trimer 2	C ₁₅ H ₂₅ N ₅ O _n (n=20-22)	ROOR	Dimer R3+M1; Dimer R1+M2
Trimer 3	C ₁₅ H ₂₅ N ₃ O _n (n=12-20)	ROOR	Dimer R2+M1; Dimer R4+M2
Trimer 4	C ₁₅ H ₂₆ N ₄ O _n (n=17-21)	ROOR	Dimer R2+M2

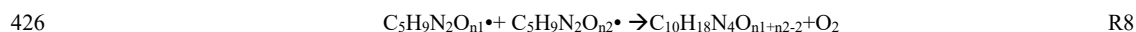
416 ^a: ROOR denotes for organic peroxide.

417 ^b: The numbering is referred to Table 1.

418 A number of HOM dimer series were observed, including C₁₀H₁₆N₂O_n (n=10-17), C₁₀H₁₇N₃O_n (n=11-19), and
419 C₁₀H₁₈N₄O_n (n=15-18), C₁₀H₁₈N₂O_n (n=10-16), C₁₀H₁₅N₃O_n (n=14-17), and C₁₀H₁₉N₃O_n (n=14-15) series (Table 2,
420 Table S3). C₁₀H₁₆N₂O_n series (dimer 1, Table 2) was likely formed by the accretion reaction of two monomer RO₂
421 of M1a/b (Reaction R7).

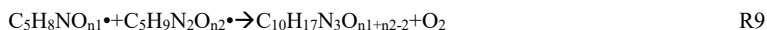


423 Similarly, C₁₀H₁₈N₄O_n series (dimer 2, Table 2) were likely formed by the accretion reaction of two monomer RO₂
424 of M2 (Reaction R8). As n₁ and n₂ are ≥ 9, the number of oxygen in C₁₀H₁₈N₄O_n is expected to be ≥16. This is
425 consistent with our observation that only C₁₀H₁₈N₄O_n with n≥16 had significant concentrations.



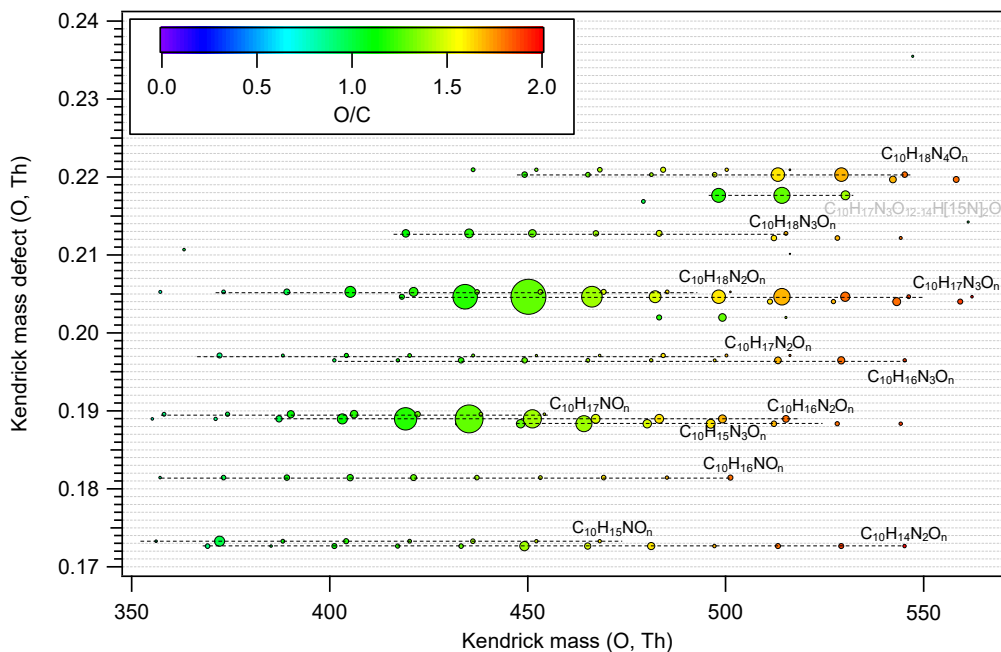


427 $C_{10}H_{17}N_3O_n$ series (dimer 3, Table 2) were likely formed by the cross accretion reaction of one M1 RO₂ and one
428 M2 RO₂ (reaction R9). Since n_1 is ≥ 5 and n_2 is ≥ 9 , the number of oxygen atoms in $C_{10}H_{17}N_3O_n$ is expected to be
429 ≥ 12 , which is also roughly consistent with our observation that only $C_{10}H_{17}N_3O_n$ with $n \geq 11$ were detected.



431 Similarly, $C_{10}H_{18}N_2O_n$ ($n=10-16$) and $C_{10}H_{15}N_3O_n$ ($n=14-17$) series (dimer 4, dimer 5, Table 2) were likely formed
432 from the accretion reaction of one M1 RO₂ and one M4 RO₂, and of one M1 RO₂ and one M3 RO₂ ($C_5H_7N_2O_9 \bullet$).
433 Other dimer series than dimer 1-5 were also present. However, they had quite low intensity (Fig. 4), which was
434 consistent with the low abundance of their parent monomer RO₂. They can be formed from various accretion reactions
435 of monomer RO₂. For example, $C_{10}H_{19}N_3O_n$ can be formed by the accretion reaction of $C_5H_9N_2O_n \bullet$ and $C_5H_{10}NO_n \bullet$
436 (Table 2).

437 Similar to monomers, few species dominated in HOM dimers spectrum. The dominant dimer series were
438 $C_{10}H_{17}N_3O_x$ and $C_{10}H_{16}N_2O_x$ series, with $C_{10}H_{17}N_3O_{12-14}$ and $C_{10}H_{16}N_2O_{12-14}$ showing highest intensity among each
439 series (Fig. 4). In addition, the O/C ratio or oxidation state of HOM dimers were generally lower than that of
440 monomers (Fig. 2, Fig. 4), which resulted from the loss of two oxygen atoms in the accretion reaction of two
441 monomer RO₂.



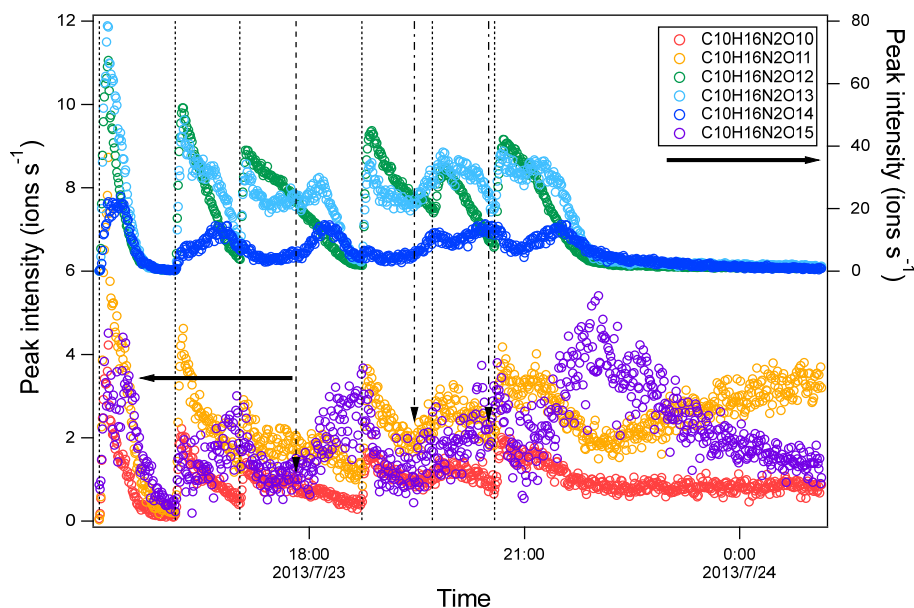
442
443 Figure 4. Kendrick mass defect plot for O of HOM dimers formed in isoprene+NO₃. The size (area) of circles is
444 set to be proportional to the average peak intensity of each molecular formula during the first isoprene addition period
445 (P1).

446 According to the mechanism above (R7-9), we attempt to explain the relative intensities of the dimers using
447 the signal intensities of monomer RO₂. Assuming that the rate constant for each of HOM-RO₂+ HOM-RO₂ reaction
448 forming dimers is the same considering that all HOM-RO₂ are highly oxygenated with a number of functional groups,



449 it is expected that the dimer formed by the recombination of the most abundant RO₂ has the highest intensity.
450 The most abundant monomer RO₂ were C₅H₉N₂O₉• and C₅H₉N₂O₁₀• and thus the most abundant dimers are expected
451 to be C₁₀H₁₆N₄O₁₆, C₁₀H₁₆N₄O₁₇, and C₁₀H₁₆N₄O₁₈. This expected result is in contrast with our observation showing
452 that the most abundant dimers were C₁₀H₁₇N₃O₁₂₋₁₄ and C₁₀H₁₆N₂O₁₂₋₁₄ (Fig. 4). The discrepancy is possibly
453 attributed to the presence of less oxygenated RO₂ (with O₅) that have a low detection sensitivity in the NO₃-CIMS
454 (Riva et al., 2019) due to their lower oxygenation compared with other HOM RO₂ shown above. These RO₂ may
455 react with C₅H₉N₂O₉• and C₅H₉N₂O₁₀•. For example, C₅H₈NO₅• (RO₂) is proposed to be an important first-
456 generation RO₂ in the oxidation of isoprene by NO₃ (Ng et al., 2008; Rollins et al., 2009; Kwan et al., 2012;
457 Schwantes et al., 2015). Although C₅H₈NO₅• showed very low signal in our mass spectra, it was likely to have high
458 abundance since it was the first RO₂ formed in the reaction of isoprene with NO₃. Indeed we found that the
459 termination products of C₅H₈NO₅• such as C₅H₉NO₅, C₅H₇NO₄, and C₅H₉NO₄ had high abundance in another study
460 (Wu et al., 2020), indicating the high abundance of C₅H₈NO₅•. The accretion reaction of C₅H₈NO₅• with C₅H₈N₂O₉-
461 10• and C₅H₈NO₅-10• can explain the high abundance of C₁₀H₁₇N₃O₁₂₋₁₄ and C₁₀H₁₆N₂O₁₂₋₁₄ among all dimers.

462 Provided that C₅H₈NO₅• is abundant, we still cannot explain the relative intensity of C₁₀H₁₇N₃O₁₂,
463 C₁₀H₁₇N₃O₁₃, and C₁₀H₁₇N₃O₁₄ that were all formed by the accretion reaction with C₅H₈NO₅•. C₁₀H₁₇N₃O₁₂ should
464 have the highest intensity among C₁₀H₁₇N₃O₁₂₋₁₄ as its precursor RO₂, C₅H₉N₂O₉•, is the most abundant. This
465 suggests that accretion reactions other than those of C₅H₈NO₅• with C₅H₈N₂O₉₋₁₀• also contributed to C₁₀H₁₇N₃O₁₂-
466 14.



467
468 Figure 5. Time series of peak intensity of several HOM dimers of C₁₀H₁₆N₂O_n series. The dashed lines indicate the
469 time of isoprene additions. The long-dashed arrow indicates the time of NO₂ addition. The dash-dotted arrows
470 indicate the time of O₃ additions. The horizontal arrows indicate y-axis scales for different markers.



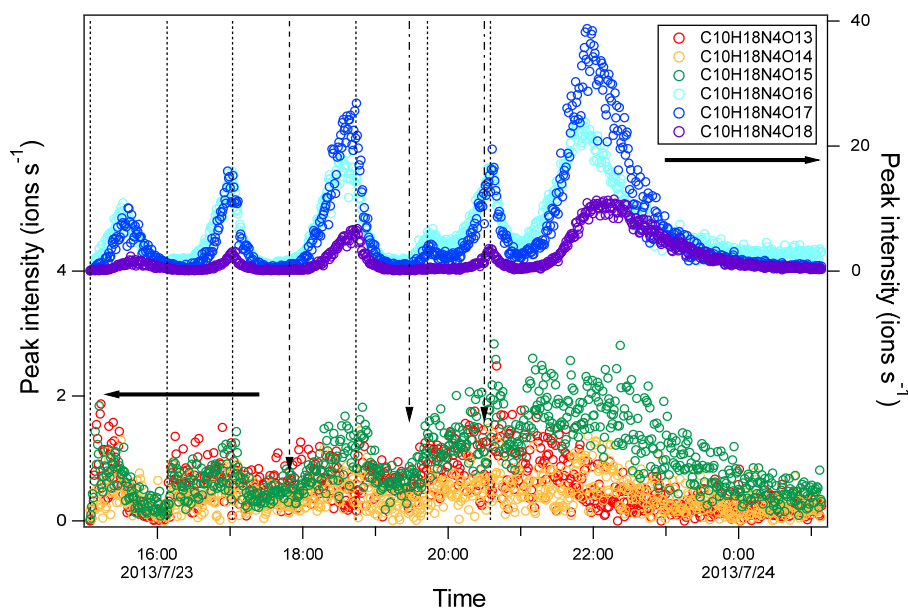
471 The time profiles of $C_{10}H_{16}N_2O_n$ indicate contributions of both the first- and second-generation products.
472 The dominance of the first- or second-generation products depended on the specific compounds. Most $C_{10}H_{16}N_2O_n$
473 compounds increased instantaneously after isoprene additions, indicating significant contributions of first-generation
474 products. Since the formation of $C_{10}H_{16}N_2O_n$ likely involved $C_5H_8NO_5^\bullet$ as discussed above, the instantaneous
475 increase may result from the increase of $C_5H_8NO_5^\bullet$ as well as other first-generation RO_2 . After the initial increase,
476 $C_{10}H_{16}N_2O_{10-12}$ then decayed with time (Fig. 5) while $C_{10}H_{16}N_2O_{13-15}$ increased again in the later phase of a period
477 besides when NO_2 and O_3 were added. The second increase indicated that $C_{10}H_{16}N_2O_{13-15}$ may contain more than
478 one isomers, which had different production pathways. As discussed above, $C_5H_8NO_n^\bullet$ can be either a first-
479 generation RO_2 formed directly via the reaction of isoprene with NO_3 and autoxidation, or a second-generation RO_2 ,
480 e.g. formed via the reaction of with $C_5H_8O_2$ with NO_3 . Therefore the second increase of $C_{10}H_{16}N_2O_{13-15}$ may result
481 from the reaction of two first-generation RO_2 and of two second-generation RO_2 or between one first-generation
482 and one second-generation RO_2 . The increase of $C_{10}H_{16}N_2O_{14-15}$ after isoprene addition was not obvious,
483 indicating the larger contributions from second-generation products compared with other $C_{10}H_{16}N_2O_n$. Overall,
484 as the number of oxygen increased, the contribution of second-generation products to $C_{10}H_{16}N_2O_n$ increased.

485 In contrast to $C_{10}H_{16}N_2O_n$ series, $C_{10}H_{18}N_4O_n$ increased gradually after each isoprene addition and then
486 decreased afterward (Fig. 6), either naturally or after isoprene additions, which is typical for second-generation
487 products. Since $C_{10}H_{18}N_4O_n$ was likely formed by the accretion reaction of $C_5H_9N_2O_n^\bullet$ (RO_2), the time profile
488 of $C_{10}H_{18}N_4O_n$ was as expected since $C_5H_9N_2O_n^\bullet$ was formed via the reaction of NO_3 with first-generation
489 products $C_5H_9NO_n$. The $C_{10}H_{18}N_4O_n$ concentration depended on the product of the concentrations of two
490 $C_5H_9N_2O_n^\bullet$. Taking $C_{10}H_{18}N_4O_{16}$ as an example, its concentration can be expressed as follows:

$$491 \quad \frac{d[C_{10}H_{18}N_4O_{16}]}{dt} = k[C_5H_9N_2O_9][C_5H_9N_2O_9] - k_w[C_{10}H_{18}N_4O_{16}]$$

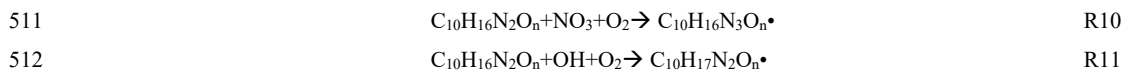
492 When the concentration of $C_5H_9N_2O_9^\bullet$ increased, the changing rate of $C_{10}H_{18}N_4O_{16}$ was positive and increased
493 and thus the concentration of $C_{10}H_{18}N_4O_{16}$ increased. When the concentration $C_5H_9N_2O_9^\bullet$ decreased sharply
494 after isoprene additions, the changing rate of $C_{10}H_{18}N_4O_{16}$ decreased and even became negative values, and thus
495 the concentration of $C_{10}H_{18}N_4O_{16}$ decreased after isoprene addition.

496 Similar to the $C_{10}H_{16}N_2O_n$ series, while $C_{10}H_{17}N_3O_n$ first increased instantaneously with isoprene
497 addition, it increased again during the later stage of each period (Fig. S9), showing a mixed behavior of the first-
498 generation products and second-generation products. The time series of $C_{10}H_{17}N_3O_n$ was as expected in general
499 because $C_{10}H_{17}N_3O_n$ was likely formed via the accretion reaction of $C_5H_8NO_n^\bullet$ (M1 RO_2) and $C_5H_9N_2O_n^\bullet$ (M2
500 RO_2), which were first- or second-generation, and second-generation RO_2 , respectively,

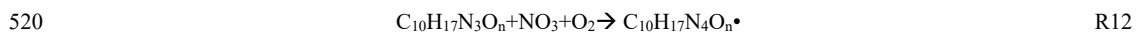


501
 502 Figure 6. Time series of peak intensity of several HOM dimers of $C_{10}H_{18}N_4O_n$ series. The dashed lines indicate the
 503 time of isoprene additions. The long-dashed arrow indicates the time of NO_2 addition. The dash-dotted arrows
 504 indicate the time of O_3 additions. The horizontal arrows indicate y-axis scales for different markers.

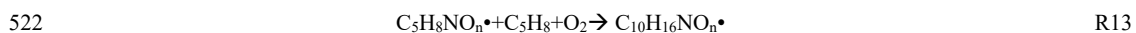
505 Some dimers that cannot be explained by accretion reactions such as $C_{10}H_{16}N_3O_n$ ($n=12-15$), $C_{10}H_{17}N_2O_n$,
 506 $C_{10}H_{16}NO_n$ ($n=10-16$), $C_{10}H_{15}NO_n$ ($n=9-12$), $C_{10}H_{17}NO_n$ ($n=11-19$) were also observed. These dimers had low abundance.
 507 Since $C_{10}H_{16}NO_n$ ($n=10-16$), $C_{10}H_{16}N_3O_n$ ($n=12-15$), and $C_{10}H_{17}N_2O_n$ contain unpaired electrons, they cannot be formed
 508 via the direct accretion reaction of two RO_2 . $C_{10}H_{16}N_3O_n$ (dimer R1) and $C_{10}H_{17}N_2O_n$ (dimer R2) were
 509 likely RO_2 formed by the reaction of HOM dimers containing a double bond (dimer 1) with NO_3 and with OH,
 510 respectively, followed by the reaction with O_2 .



513 The corresponding termination products of $C_{10}H_{16}N_3O_n \cdot RO_2$ series such as $C_{10}H_{15}N_3O_n$ (ketone), $C_{10}H_{17}N_3O_n$
 514 (hydroperoxide/alcohol) were also observed, although these compounds can also be formed via reactions between
 515 two RO_2 radicals (R9 and R11). Among the termination products, $C_{10}H_{15}N_3O_n$ had low intensity. Reaction R13 and
 516 the termination reaction of $C_{10}H_{17}N_2O_n \cdot$ with HO_2 provided an additional pathway to $C_{10}H_{17}N_3O_n$ besides the R9
 517 pathway discussed above. Similarly, other dimers may also be formed by the termination reactions of dimer RO_2
 518 with RO_2 or HO_2 . E.g., $C_{10}H_{18}N_4O_n$ can be formed via termination reaction of $C_{10}H_{17}N_4O_n \cdot$ with another RO_2 wherein
 519 $C_{10}H_{17}N_4O_n \cdot$ can be formed as follows:



521 $C_{10}H_{16}NO_n$ ($n=10-16$) could be explained by the reaction of monomer RO_2 with isoprene.





523 It seems that only $C_5H_8NO_n^*$ with more than eight oxygen atoms reacted with isoprene, because only $C_{10}H_{16}NO_n$ with
524 $n > 8$ were detected. Such a reaction of RO_2 with isoprene has been proposed by Ng et al. (2008) and Kwan et al.
525 (2012). The corresponding termination products of $C_{10}H_{16}NO_n^*$ are $C_{10}H_{15}NO_n$ (ketone) and $C_{10}H_{17}NO_n$ species
526 (hydroperoxide/alcohol). $C_{10}H_{17}NO_n$ species showed a time profile of typical first-generation products (Fig. S10), i.e.
527 increasing immediately with isoprene addition and then decaying with time. This behaviour further supports the
528 possibility of reaction R13. Yet, the reaction rate of alkene with RO_2 is likely low due to the high activation energy
529 (Stark, 1997, 2000). It is worth noting that to our knowledge no kinetic data on the addition of RO_2 to alkenes in the
530 gas phase in atmospheric relevant conditions are available, though fast, low-barrier ring closure reactions in
531 unsaturated RO_2 radicals have been reported (Vereecken and Peeters, 2004, 2012; Kaminski et al., 2017; Richters et
532 al., 2017).

533 Some of the dimers discussed above have been observed in previous studies. Ng et al. (2008) found
534 $C_{10}H_{16}N_2O_8$ and $C_{10}H_{16}N_2O_9$ in the gas phase and $C_{10}H_{17}N_3O_{12}$, $C_{10}H_{17}N_3O_{13}$, $C_{10}H_{18}N_4O_{16}$, and $C_{10}H_{17}N_5O_{18}$ in the
535 particle phase. $C_{10}H_{16}N_2O_8$ and $C_{10}H_{16}N_2O_9$ were also observed in our study, but their intensity in the MS was too
536 low to assign molecular formulas with high confidence. The low intensity may be due to the low sensitivity of
537 $C_{10}H_{16}N_2O_8$, 9 in NO_3^- -CIMS. According to modelling results of the products formed in cyclohexene ozonolysis by
538 Hyttinen et al. (2015), at least two hydrogen bond donor functional groups are needed for a compound to be detected
539 in a nitrate CIMS. As $C_{10}H_{16}N_2O_8$ and $C_{10}H_{16}N_2O_9$ have no and only one H-bond donor function groups, respectively,
540 they are expected to have low sensitivity in NO_3^- -CIMS. Moreover, the low intensity can be partly attributed to the
541 much lower isoprene concentrations used in this study compared to previous studies, leading to the low concentration
542 of $C_{10}H_{16}N_2O_8$ and $C_{10}H_{16}N_2O_9$ (Ng et al., 2008). $C_{10}H_{17}N_3O_{12}$, $C_{10}H_{17}N_3O_{13}$, $C_{10}H_{18}N_4O_{16}$, and $C_{10}H_{17}N_5O_{18}$ were
543 all observed in the gas phase in this study, wherein the concentration of $C_{10}H_{17}N_5O_{18}$ was very low. The formation
544 pathways of $C_{10}H_{17}N_3O_{12}$, $C_{10}H_{17}N_3O_{13}$, and $C_{10}H_{18}N_4O_{16}$ (R8) were generally similar to those proposed by Ng et al.
545 (2008) except that the products from H-shift of RO_2 were involved in the formation of $C_{10}H_{17}N_3O_{13}$. Among the two
546 pathways of $C_{10}H_{18}N_4O_{16}$ formation (R8 and via R12), our results indicate that R8 was the main pathway, based on
547 the low concentrations of $C_{10}H_{17}N_4O_{16/17}^*$ and other termination product of them, $C_{10}H_{16}N_4O_{15/16}$. That the time
548 profile of $C_{10}H_{18}N_4O_{16}$ was consistent with what is expected from R8 as discussed above offers additional evidence
549 to that conclusion.

550 3.4 HOM trimers and their formation

551 A series of HOM trimers were observed, such as $C_{15}H_{24}N_4O_n$ ($n=17-23$), $C_{15}H_{25}N_5O_n$ ($n=20-22$), $C_{15}H_{25}N_3O_n$
552 ($n=12-20$), $C_{15}H_{26}N_4O_n$ ($n=17-21$), and $C_{15}H_{24}N_2O_n$ ($n=12-16$). Among trimers, $C_{15}H_{24}N_4O_n$ ($n=17-23$) was the most abundant
553 series (Fig. S11). The $C_{15}H_{24}N_4O_n$ series can be explained by the accretion reaction of one monomer HOM RO_2
554 and one dimer HOM RO_2 .



556 The formation pathways of dimer RO_2 $C_{10}H_{16}N_3O_n$ ($n=14-20$) and $C_{10}H_{17}N_2O_n$ are shown above (reaction R14).

557 The other trimers were likely formed via similar pathways (Table 2 and Supplement S2). Since NO_3^- -CIMS
558 cannot provide the structural information of these HOM trimers, we cannot elucidate the major pathways. However,
559 in all these pathways, dimer- RO_2 is necessary to form a trimer, and most of the dimer- RO_2 formation pathways



560 require at least one double bond in the dimer molecule except for the reaction of RO₂ with isoprene. Since one
561 double bond has already reacted in the monomer-RO₂ formation, we anticipate that in the reaction with NO₃ it is
562 more favourable for precursors (VOC) containing more than one double bonds to form trimer molecules than
563 precursors containing only one double bond, as it is easier to generate new RO₂ radicals from these dimers by
564 attack on the remaining double bond(s).

565 The time profile of C₁₅H₂₄N₄O_n showed the mixed behavior of first- and second-generation products (Fig.
566 S12), consistent with the mechanism discussed above since C₅H₈NO_n• and C₁₀H₁₆N₃O_n• were of first- or second-
567 generation and second-generation, respectively. The contributions of the second-generation products became
568 larger as the number of oxygen atoms increased. In contrast, C₁₅H₂₅N₃O_n showed instantaneous increase with
569 isoprene addition (Fig. S13), which was typical for time profiles of first-generation products. Both the formation
570 pathways of C₁₅H₂₅N₃O_n (RS6 and RS7) contained a second-generation RO₂, which was not in line with the time
571 profile observed. The observation cannot be well explained, unless we assume molecular adducts of a dimer with one
572 monomer. It is also possible that some C₁₀H₁₇N₂O_n• were formed very fast or there were other formation pathways
573 of C₁₅H₂₅N₃O_n that have not been accounted for here.

574 3.5 Contributions of monomers, dimer, and trimers to HOM

575 The concentration (represented by peak intensity) of monomers was higher than that of dimers, but overall
576 their concentrations remained of the same order of magnitude (Fig 1a, inset). The concentration of trimers was much
577 lower than that of monomers and dimers. The relative contributions of monomers, dimers, and trimers evolved in
578 time due to the changing concentration of each HOM species. Comparing the contributions of various classes of
579 HOM in period 1 with those in periods 1-6 reveals that the relative contribution of monomers increased with time,
580 especially that of 2N-monomers, while the contribution of dimers decreased. This trend is attributed to the larger wall
581 loss of dimers compared to monomers because of their lower volatility and also to the continuous formation of
582 second-generation monomers, mostly 2N-monomers. Overall, the relative contribution of total HOM monomers
583 decreased immediately after isoprene addition while the contribution of HOM dimers increased rapidly (Fig. S14),
584 which was attributed to the faster increase of dimers intensity due to their rapid formation. Afterwards, the
585 contribution of monomers to total HOM gradually increased and that of dimers decreased, which was partly due to
586 the faster wall loss rate of dimers and to the continuous formation of second-generation monomers.

587 3.6 Yield of HOM

588 The HOM yield in the oxidation of isoprene by NO₃ was estimated to be 1.2%^{+1.3%}_{-0.7%} using the sensitivity of
589 H₂SO₄ (Pullinen et al., 2020). The uncertainty was estimated as shown in the Supplement S1. Despite the uncertainty,
590 the HOM yield here was much higher than the yield from the ozonolysis and photooxidation of isoprene (Jokinen et
591 al., 2015). The difference may be attributed to the more efficient oxygenation in the addition of NO₃ to carbon double
592 bonds. Compared with the reaction with O₃ or OH, the initial peroxy radicals contains 5 oxygen atoms when isoprene
593 reacts with NO₃, while the initial peroxy radicals contains only 3 oxygen atoms when reacting with OH, and the
594 ozonide contains 3 oxygen atoms in the case of O₃.



595 4 Conclusion and implications

596 HOM formation in the reaction of isoprene with NO₃ was investigated in the SAPHIR chamber. A number
597 of HOM monomers, dimers, and trimers containing one to five nitrogen atoms were detected and their time-dependent
598 concentration profiles were tracked throughout the experiment. The formation mechanisms of various HOM were
599 proposed according to the molecular formula identified, and the available literature. HOM showed a variety of time
600 profiles with multiple isoprene additions during the reaction. First-generation HOM increased instantaneously after
601 isoprene addition and then decreased while second-generation HOM increased gradually and then decreased with
602 time, reaching a maximum at the later stage of each period. The time profiles provide additional constraints on their
603 formation mechanism beside the molecular formula, suggesting whether they were first-generation products or
604 second-generation products. 1N-monomers (mostly C₅) were likely formed by NO₃ addition to a double bond of
605 isoprene, forming monomer RO₂, followed by autoxidation and termination via the reaction with HO₂, RO₂, and NO₃.
606 Time series suggest that some 1N-monomer could also be formed by the reaction of first-generation products with
607 NO₃, and thus be of second-generation. 2N-monomers were likely formed via the reaction of first-generation products
608 such as C₅-hydroxynitrate with NO₃ and thus second-generation products. 3N-monomers likely comprised
609 peroxy/peroxyacyl nitrates formed by the reaction of 2N-monomer RO₂ with NO₂, and nitronitrates formed via the
610 direct addition of N₂O₅ to the first-generation products. HOM dimers were mostly formed by the accretion reactions
611 between various HOM monomer RO₂, either first-generation or second-generation or with the contributions of both,
612 and thus showed time profiles typical of either first- generation products, or second-generation products, or a mixture
613 of both. Additionally, some dimers were formed by the reaction of dimer with NO₃ forming dimer RO₂. HOM trimers
614 were proposed to be formed by accretion reactions between the monomer RO₂ and dimer RO₂, the latter formed by
615 the reaction of NO₃ with dimers containing a C=C double bond.

616 Overall, both HOM monomers and dimers contribute significantly to total HOM while trimers only
617 contributed a minor fraction. Within both the monomer and dimer compounds, a limited set of compounds dominated
618 the abundance, such as C₅H₈N₂O_n, C₅H₁₀N₂O_n, C₁₀H₁₇N₃O_n, and C₁₀H₁₆N₂O_n series. 2N-monomers, which were
619 second-generation products, dominated in monomers and accounted for ~34% of all HOM, indicating the important
620 role of second-generation oxidation in HOM formation in isoprene+NO₃. Both RO₂ autoxidation and “alkoxy-peroxy”
621 pathways were found to be important for 1N- and 2N-HOM formation. In total, the yield of HOM monomers, dimers,
622 and trimers accounted for 1.3%^{+1.3%}_{-0.7%} of the isoprene reacted, which was much higher than the HOM yield in the
623 oxidation of isoprene by OH and O₃ reported in the literature. This means that the reaction of isoprene with NO₃ is a
624 competitive pathway of HOM formation from isoprene.

625 The HOM in the reaction of isoprene with NO₃ may account for a significant fraction of SOA. If all the
626 HOM condense on particles, using the molecular weight of the HOM with the least molecular weight observed in
627 this study (C₅H₉NO₆), the HOM yield corresponds to a SOA yield of 3.6%. Although SOA concentrations were not
628 measured in this study, Ng et al. (2008) reported a SOA yield of isoprene+NO₃ of 4.3%-23.8%. Rollins et al. (2009)
629 reported a SOA yield of 2% at low organic aerosol loading (~0.52 μg m⁻³) and 14% if the further oxidation of the
630 first-generation products are considered in isoprene+NO₃. Comparing the potential SOA yield produced by HOM
631 with SOA yield in the literature suggests that HOM may play an important role in the SOA formation in
632 isoprene+NO₃.



633 **Data availability**

634 All the data in the figures of this study are available upon request to the corresponding author (t.mentel@fz-juelich.
635 de).

636 **Competing interests**

637 The authors declare that they have no conflict of interest.

638 **Author contribution**

639 TFM, HF, SS, DZ, IP, AW, and AKS designed the experiments. Instrument deployment and operation were carried
640 out by IP, HF, SS, IA, RT, FR, DZ, and RW. Data analysis was done by DZ, HF, SS, RW, IA, RT, FR, YG, SK. DZ,
641 TFM, RW, JW, SK, and LV interpreted the compiled data set. DZ and TFM wrote the paper. All co-authors discussed
642 the results and commented on the paper.

643 **Acknowledgements**

644 We thank the SAPHIR team for supporting our measurements and providing helpful data. D. Zhao and Y. Guo would
645 like to thank the support of National Natural Science Foundation of China (41875145).



References

- Atkinson, R., Baulch, D. L., Cox, R. A., Crowley, J. N., Hampson, R. F., Hynes, R. G., Jenkin, M. E., Rossi, M. J., and Troe, J.: Evaluated kinetic and photochemical data for atmospheric chemistry: Volume II - gas phase reactions of organic species, *Atmos. Chem. Phys.*, 6, 3625-4055, 2006.
- Ayres, B. R., Allen, H. M., Draper, D. C., Brown, S. S., Wild, R. J., Jimenez, J. L., Day, D. A., Campuzano-Jost, P., Hu, W., de Gouw, J., Koss, A., Cohen, R. C., Duffey, K. C., Romer, P., Baumann, K., Edgerton, E., Takahama, S., Thornton, J. A., Lee, B. H., Lopez-Hilfiker, F. D., Mohr, C., Wennberg, P. O., Nguyen, T. B., Teng, A., Goldstein, A. H., Olson, K., and Fry, J. L.: Organic nitrate aerosol formation via NO_3 + biogenic volatile organic compounds in the southeastern United States, *Atmos. Chem. Phys.*, 15, 13377-13392, 10.5194/acp-15-13377-2015, 2015.
- Berndt, T., and Böge, O.: Gas-phase reaction of NO_3 radicals with isoprene: a kinetic and mechanistic study, *Int. J. Chem. Kinet.*, 29, 755-765, 10.1002/(sici)1097-4601(1997)29:10<755::Aid-kin4>3.0.Co;2-I, 1997.
- Berndt, T., Mender, B., Scholz, W., Fischer, L., Herrmann, H., Kulmala, M., and Hansel, A.: Accretion Product Formation from Ozonolysis and OH Radical Reaction of alpha-Pinene: Mechanistic Insight and the Influence of Isoprene and Ethylene, *Environ. Sci. Technol.*, 52, 11069-11077, 10.1021/acs.est.8b02210, 2018a.
- Berndt, T., Scholz, W., Mentler, B., Fischer, L., Herrmann, H., Kulmala, M., and Hansel, A.: Accretion Product Formation from Self- and Cross-Reactions of RO_2 Radicals in the Atmosphere, *Angew. Chem.-Int. Edit.*, 57, 3820-3824, 10.1002/anie.201710989, 2018b.
- Bianchi, F., Kurten, T., Riva, M., Mohr, C., Rissanen, M. P., Roldin, P., Berndt, T., Crouse, J. D., Wennberg, P. O., Mentel, T. F., Wildt, J., Junninen, H., Jokinen, T., Kulmala, M., Worsnop, D. R., Thornton, J. A., Donahue, N., Kjaergaard, H. G., and Ehn, M.: Highly Oxygenated Organic Molecules (HOM) from Gas-Phase Autoxidation Involving Peroxy Radicals: A Key Contributor to Atmospheric Aerosol, *Chem. Rev.*, 119, 3472-3509, 10.1021/acs.chemrev.8b00395, 2019.
- Boyd, C. M., Sanchez, J., Xu, L., Eugene, A. J., Nah, T., Tuet, W. Y., Guzman, M. I., and Ng, N. L.: Secondary organic aerosol formation from the beta-pinene+ NO_3 system: effect of humidity and peroxy radical fate, *Atmos. Chem. Phys.*, 15, 7497-7522, 10.5194/acp-15-7497-2015, 2015.
- Boyd, C. M., Nah, T., Xu, L., Berkemeier, T., and Ng, N. L.: Secondary Organic Aerosol (SOA) from Nitrate Radical Oxidation of Monoterpenes: Effects of Temperature, Dilution, and Humidity on Aerosol Formation, Mixing, and Evaporation, *Environ. Sci. Technol.*, 51, 7831-7841, 10.1021/acs.est.7b01460, 2017.
- Brown, S. S., deGouw, J. A., Warneke, C., Ryerson, T. B., Dube, W. P., Atlas, E., Weber, R. J., Peltier, R. E., Neuman, J. A., Roberts, J. M., Swanson, A., Flocke, F., McKeen, S. A., Brioude, J., Sommariva, R., Trainer, M., Fehsenfeld, F. C., and Ravishankara, A. R.: Nocturnal isoprene oxidation over the Northeast United States in summer and its impact on reactive nitrogen partitioning and secondary organic aerosol, *Atmos. Chem. Phys.*, 9, 3027-3042, 10.5194/acp-9-3027-2009, 2009.
- Brown, S. S., Dube, W. P., Peischl, J., Ryerson, T. B., Atlas, E., Warneke, C., de Gouw, J. A., Hekkert, S. t. L., Brock, C. A., Flocke, F., Trainer, M., Parrish, D. D., Fehsenfeld, F. C., and Ravishankara, A. R.: Budgets for nocturnal VOC oxidation by nitrate radicals aloft during the 2006 Texas Air Quality Study, *J. Geophys. Res.-Atmos.*, 116, 10.1029/2011jd016544, 2011.
- Clafin, M. S., and Ziemann, P. J.: Identification and Quantitation of Aerosol Products of the Reaction of β -Pinene with NO_3 Radicals and Implications for Gas- and Particle-Phase Reaction Mechanisms, *The Journal of Physical Chemistry A*, 122, 3640-3652, 10.1021/acs.jpca.8b00692, 2018.
- Crouse, J. D., Nielsen, L. B., Jorgensen, S., Kjaergaard, H. G., and Wennberg, P. O.: Autoxidation of Organic Compounds in the Atmosphere, *J. Phys. Chem. Lett.*, 4, 3513-3520, 10.1021/jz4019207, 2013.
- Draper, D. C., Myllys, N., Hyttinen, N., Moller, K. H., Kjaergaard, H. G., Fry, J. L., Smith, J. N., and Kurten, T.: Formation of Highly Oxidized Molecules from NO_3 Radical Initiated Oxidation of Delta-3-Carene: A Mechanistic Study, *Acs Earth and Space Chemistry*, 3, 1460-1470, 10.1021/acsearthspacechem.9b00143, 2019.
- Ehn, M., Thornton, J. A., Kleist, E., Sipila, M., Junninen, H., Pullinen, I., Springer, M., Rubach, F., Tillmann, R., Lee, B., Lopez-Hilfiker, F., Andres, S., Acir, I. H., Rissanen, M., Jokinen, T., Schobesberger, S., Kangasluoma, J., Kontkanen, J., Nieminen, T., Kurten, T., Nielsen, L. B., Jorgensen, S., Kjaergaard, H. G., Canagaratna, M., Dal Maso, M., Berndt, T., Petaja, T., Wahner, A., Kerminen, V. M., Kulmala, M., Worsnop, D. R., Wildt, J., and Mentel, T. F.: A large source of low-volatility secondary organic aerosol, *Nature*, 506, 476-479, 10.1038/nature13032, 2014.



Ehn, M., Berndt, T., Wildt, J., and Mentel, T.: Highly Oxygenated Molecules from Atmospheric Autoxidation of Hydrocarbons: A Prominent Challenge for Chemical Kinetics Studies, *Int. J. Chem. Kinet.*, 49, 821-831, 10.1002/kin.21130, 2017.

Faxon, C., Hammes, J., Le Breton, M., Pathak, R. K., and Hallquist, M.: Characterization of organic nitrate constituents of secondary organic aerosol (SOA) from nitrate-radical-initiated oxidation of limonene using high-resolution chemical ionization mass spectrometry, *Atmos. Chem. Phys.*, 18, 5467-5481, 10.5194/acp-18-5467-2018, 2018.

Finlayson-Pitts, B., and Pitts, J.: *Chemistry of the upper and lower atmosphere*, Academic Press, San Diego, 2000.

Fry, J. L., Kiendler-Scharr, A., Rollins, A. W., Wooldridge, P. J., Brown, S. S., Fuchs, H., Dube, W., Mensah, A., dal Maso, M., Tillmann, R., Dorn, H. P., Brauers, T., and Cohen, R. C.: Organic nitrate and secondary organic aerosol yield from NO₃ oxidation of beta-pinene evaluated using a gas-phase kinetics/aerosol partitioning model, *Atmos. Chem. Phys.*, 9, 1431-1449, 2009.

Fry, J. L., Kiendler-Scharr, A., Rollins, A. W., Brauers, T., Brown, S. S., Dorn, H. P., Dube, W. P., Fuchs, H., Mensah, A., Rohrer, F., Tillmann, R., Wahner, A., Wooldridge, P. J., and Cohen, R. C.: SOA from limonene: role of NO₃ in its generation and degradation, *Atmos. Chem. Phys.*, 11, 3879-3894, 10.5194/acp-11-3879-2011, 2011.

Fry, J. L., Draper, D. C., Barsanti, K. C., Smith, J. N., Ortega, J., Winkle, P. M., Lawler, M. J., Brown, S. S., Edwards, P. M., Cohen, R. C., and Lee, L.: Secondary Organic Aerosol Formation and Organic Nitrate Yield from NO₃ Oxidation of Biogenic Hydrocarbons, *Environ. Sci. Technol.*, 48, 11944-11953, 10.1021/es502204x, 2014.

Fuchs, H., Dorn, H. P., Bachner, M., Bohn, B., Brauers, T., Gomm, S., Hofzumahaus, A., Holland, F., Nehr, S., Rohrer, F., Tillmann, R., and Wahner, A.: Comparison of OH concentration measurements by DOAS and LIF during SAPHIR chamber experiments at high OH reactivity and low NO concentration, *Atmos. Meas. Tech.*, 5, 1611-1626, 10.5194/amt-5-1611-2012, 2012.

Garmash, O., Rissanen, M. P., Pullinen, I., Schmitt, S., Kausiala, O., Tillmann, R., Percival, C., Bannan, T. J., Priestley, M., Hallquist, Å. M., Kleist, E., Kiendler-Scharr, A., Hallquist, M., Berndt, T., McFiggans, G., Wildt, J., Mentel, T., and Ehn, M.: Multi-generation OH oxidation as a source for highly oxygenated organic molecules from aromatics, *Atmos. Chem. Phys. Discuss.*, 2019, 1-33, 10.5194/acp-2019-582, 2019.

Geyer, A., Alicke, B., Konrad, S., Schmitz, T., Stutz, J., and Platt, U.: Chemistry and oxidation capacity of the nitrate radical in the continental boundary layer near Berlin, *J. Geophys. Res.-Atmos.*, 106, 8013-8025, 10.1029/2000jd900681, 2001.

Hyttinen, N., Kupiainen-Määttä, O., Rissanen, M. P., Muuronen, M., Ehn, M., and Kurtén, T.: Modeling the Charging of Highly Oxidized Cyclohexene Ozonolysis Products Using Nitrate-Based Chemical Ionization, *The Journal of Physical Chemistry A*, 119, 6339-6345, 10.1021/acs.jpca.5b01818, 2015.

Japar, S. M., and Niki, H.: Gas-phase reactions of the nitrate radical with olefins, *The Journal of Physical Chemistry*, 79, 1629-1632, 10.1021/j100583a002, 1975.

Jokinen, T., Sipila, M., Richters, S., Kerminen, V. M., Paasonen, P., Stratmann, F., Worsnop, D., Kulmala, M., Ehn, M., Herrmann, H., and Berndt, T.: Rapid Autoxidation Forms Highly Oxidized RO₂ Radicals in the Atmosphere, *Angew. Chem.-Int. Edit.*, 53, 14596-14600, 10.1002/anie.201408566, 2014.

Jokinen, T., Berndt, T., Makkonen, R., Kerminen, V. M., Junninen, H., Paasonen, P., Stratmann, F., Herrmann, H., Guenther, A. B., Worsnop, D. R., Kulmala, M., Ehn, M., and Sipila, M.: Production of extremely low volatile organic compounds from biogenic emissions: Measured yields and atmospheric implications, *Proc. Nat. Acad. Sci. U.S.A.*, 112, 7123-7128, 10.1073/pnas.1423977112, 2015.

Kaminski, M., Fuchs, H., Acir, I.-H., Bohn, B., Brauers, T., Dorn, H.-P., Haeseler, R., Hofzumahaus, A., Li, X., Lutz, A., Nehr, S., Rohrer, F., Tillmann, R., Vereecken, L., Wegener, R., and Wahner, A.: Investigation of the beta-pinene photooxidation by OH in the atmosphere simulation chamber SAPHIR, *Atmos. Chem. Phys.*, 17, 6631-6650, 10.5194/acp-17-6631-2017, 2017.

Kenseth, C. M., Huang, Y. L., Zhao, R., Dalleska, N. F., Hethcox, C., Stoltz, B. M., and Seinfeld, J. H.: Synergistic O₃ + OH oxidation pathway to extremely low-volatility dimers revealed in beta-pinene secondary organic aerosol, *Proc. Nat. Acad. Sci. U.S.A.*, 115, 8301-8306, 10.1073/pnas.1804671115, 2018.

Kirby, J., Duplissy, J., Sengupta, K., Frege, C., Gordon, H., Williamson, C., Heinritzi, M., Simon, M., Yan, C., Almeida, J., Tröstl, J., Nieminen, T., Ortega, I. K., Wagner, R., Adamov, A., Amorim, A., Bernhammer, A.-K., Bianchi, F., Breitenlechner, M., Brilke, S., Chen, X., Craven, J., Dias, A., Ehrhart, S., Flagan, R. C., Franchin, A., Fuchs, C., Guida, R., Hakala, J., Hoyle, C. R., Jokinen, T., Junninen, H., Kangasluoma, J., Kim, J., Krapf, M., Kürten, A., Laaksonen, A., Lehtipalo, K., Makhmutov, V., Mathot, S., Molteni, U., Onnela, A., Peräkylä, O., Piel, F., Petäjä, T., Praplan, A. P., Pringle, K., Rap, A., Richards, N. A. D., Riipinen, I., Rissanen, M. P., Rondo, L., Sarnela, N., Schobesberger, S., Scott, C. E., Seinfeld, J. H., Sipilä, M., Steiner, G., Stozhkov, Y., Stratmann, F., Tomé, A., Virtanen, A., Vogel, A. L., Wagner, A. C., Wagner, P. E., Weingartner, E., Wimmer, D., Winkler, P. M., Ye, P., Zhang, X., Hansel, A., Dommen, J., Donahue, N. M., Worsnop, D. R., Baltensperger, U., Kulmala, M., Carslaw, K. S., and Curtius, J.: Ion-induced nucleation of pure biogenic particles, *Nature*, 533, 521-526, 10.1038/nature17953, 2016.



Krechmer, J. E., Coggon, M. M., Massoli, P., Nguyen, T. B., Crounse, J. D., Hu, W. W., Day, D. A., Tyndall, G. S., Henze, D. K., Rivera-Rios, J. C., Nowak, J. B., Kimmel, J. R., Mauldin, R. L., Stark, H., Jayne, J. T., Sipila, M., Junninen, H., St Clair, J. M., Zhang, X., Feiner, P. A., Zhang, L., Miller, D. O., Brune, W. H., Keutsch, F. N., Wennberg, P. O., Seinfeld, J. H., Worsnop, D. R., Jimenez, J. L., and Canagaratna, M. R.: Formation of Low Volatility Organic Compounds and Secondary Organic Aerosol from Isoprene Hydroxyhydroperoxide Low-NO Oxidation, *Environ. Sci. Technol.*, 49, 10330-10339, 10.1021/acs.est.5b02031, 2015.

Kwan, A. J., Chan, A. W. H., Ng, N. L., Kjaergaard, H. G., Seinfeld, J. H., and Wennberg, P. O.: Peroxy radical chemistry and OH radical production during the NO₃-initiated oxidation of isoprene, *Atmos. Chem. Phys.*, 12, 7499-7515, 10.5194/acp-12-7499-2012, 2012.

Lai, C. C., and Finlayson-Pitts, B. J.: Reactions of dinitrogen pentoxide and nitrogen-dioxide with 1-palmitoyl-2-oleoyl-sn-glycero-3-phosphocholine, *Lipids*, 26, 306-314, 10.1007/bf02537142, 1991.

Lee, B. H., Mohr, C., Lopez-Hilfiker, F. D., Lutz, A., Hallquist, M., Lee, L., Romer, P., Cohen, R. C., Iyer, S., Kurten, T., Hu, W., Day, D. A., Campuzano-Jost, P., Jimenez, J. L., Xu, L., Ng, N. L., Guo, H., Weber, R. J., Wild, R. J., Brown, S. S., Koss, A., de Gouw, J., Olson, K., Goldstein, A. H., Seco, R., Kim, S., McAvey, K., Shepson, P. B., Starn, T., Baumann, K., Edgerton, E. S., Liu, J., Shilling, J. E., Miller, D. O., Brune, W., Schobesberger, S., D'Ambro, E. L., and Thornton, J. A.: Highly functionalized organic nitrates in the southeast United States: Contribution to secondary organic aerosol and reactive nitrogen budgets, *Proc. Nat. Acad. Sci. U.S.A.*, 113, 1516-1521, 10.1073/pnas.1508108113, 2016.

McFiggans, G., Mentel, T. F., Wildt, J., Pullinen, I., Kang, S., Kleist, E., Schmitt, S., Springer, M., Tillmann, R., Wu, C., Zhao, D., Hallquist, M., Faxon, C., Le Breton, M., Hallquist, A. M., Simpson, D., Bergström, R., Jenkin, M. E., Ehn, M., Thornton, J. A., Alfarra, M. R., Bannan, T. J., Percival, C. J., Priestley, M., Topping, D., and Kiendler-Scharr, A.: Secondary organic aerosol reduced by mixture of atmospheric vapours, *Nature*, 565, 587-593, 10.1038/s41586-018-0871-y, 2019.

Mentel, T. F., Springer, M., Ehn, M., Kleist, E., Pullinen, I., Kurten, T., Rissanen, M., Wahner, A., and Wildt, J.: Formation of highly oxidized multifunctional compounds: autoxidation of peroxy radicals formed in the ozonolysis of alkenes - deduced from structure-product relationships, *Atmos. Chem. Phys.*, 15, 6745-6765, 10.5194/acp-15-6745-2015, 2015.

Moller, K. H., Bates, K. H., and Kjaergaard, H. G.: The Importance of Peroxy Radical Hydrogen-Shift Reactions in Atmospheric Isoprene Oxidation, *J. Phys. Chem. A* 123, 920-932, 10.1021/acs.jpca.8b10432, 2019.

Molteni, U., Bianchi, F., Klein, F., El Haddad, I., Frege, C., Rossi, M. J., Dommen, J., and Baltensperger, U.: Formation of highly oxygenated organic molecules from aromatic compounds, *Atmos. Chem. Phys.*, 18, 1909-1921, 10.5194/acp-18-1909-2018, 2018.

Molteni, U., Simon, M., Heinritzi, M., Hoyle, C. R., Bernhammer, A. K., Bianchi, F., Breitenlechner, M., Brilke, S., Dias, A., Duplissy, J., Frege, C., Gordon, H., Heyn, C., Jokinen, T., Kurten, A., Lehtipalo, K., Makhmutov, V., Petaja, T., Pieber, S. M., Praplan, A. P., Schobesberger, S., Steiner, G., Stozhkov, Y., Tome, A., Trostl, J., Wagner, A. C., Wagner, R., Williamson, C., Yan, C., Baltensperger, U., Curtius, J., Donahue, N. M., Hansel, A., Kirkby, J., Kulmala, M., Worsnop, D. R., and Dommen, J.: Formation of Highly Oxygenated Organic Molecules from alpha-Pinene Ozonolysis: Chemical Characteristics, Mechanism, and Kinetic Model Development, *Acs Earth and Space Chemistry*, 3, 873-883, 10.1021/acsearthspacechem.9b00035, 2019.

Nah, T., Sanchez, J., Boyd, C. M., and Ng, N. L.: Photochemical Aging of alpha-pinene and beta-pinene Secondary Organic Aerosol formed from Nitrate Radical Oxidation, *Environ. Sci. Technol.*, 50, 222-231, 10.1021/acs.est.5b04594, 2016.

Ng, N. L., Kwan, A. J., Surratt, J. D., Chan, A. W. H., Chhabra, P. S., Sorooshian, A., Pye, H. O. T., Crounse, J. D., Wennberg, P. O., Flagan, R. C., and Seinfeld, J. H.: Secondary organic aerosol (SOA) formation from reaction of isoprene with nitrate radicals (NO₃), *Atmos. Chem. Phys.*, 8, 4117-4140, 10.5194/acp-8-4117-2008, 2008.

Nguyen, T. B., Tyndall, G. S., Crounse, J. D., Teng, A. P., Bates, K. H., Schwantes, R. H., Coggon, M. M., Zhang, L., Feiner, P., Milller, D. O., Skog, K. M., Rivera-Rios, J. C., Dorris, M., Olson, K. F., Koss, A., Wild, R. J., Brown, S. S., Goldstein, A. H., de Gouw, J. A., Brune, W. H., Keutsch, F. N., Seinfeld, J. H., and Wennberg, P. O.: Atmospheric fates of Criegee intermediates in the ozonolysis of isoprene, *Phys. Chem. Chem. Phys.*, 18, 10241-10254, 10.1039/c6cp00053c, 2016.

Perring, A. E., Wisthaler, A., Graus, M., Wooldridge, P. J., Lockwood, A. L., Mielke, L. H., Shepson, P. B., Hansel, A., and Cohen, R. C.: A product study of the isoprene+NO₃ reaction, *Atmos. Chem. Phys.*, 9, 4945-4956, 10.5194/acp-9-4945-2009, 2009.

Pfrang, C., Martin, R. S., Canosa-Mas, C. E., and Wayne, R. P.: Gas-phase reactions of NO₃ and N₂O₅ with (Z)-hex-4-en-1-ol, (Z)-hex-3-en-1-ol ('leaf alcohol'), (E)-hex-3-en-1-ol, (Z)-hex-2-en-1-ol and (E)-hex-2-en-1-ol, *Phys. Chem. Chem. Phys.*, 8, 354-363, 10.1039/b510835g, 2006.

Pullinen, I., Schmitt, S., Kang, S., Sarrafzadeh, M., Schlag, P., Andres, S., Kleist, E., Mentel, T. F., Rohrer, F., Springer, M., Tillmann, R., Wildt, J., Wu, C., Zhao, D., Wahner, A., and Kiendler-Scharr, A.: Impact of NO_x on secondary organic aerosol (SOA) formation from alpha-pinene and beta-pinene photooxidation: the role of highly oxygenated organic nitrates, *Atmos. Chem. Phys.*, 20, 10125-10147, 10.5194/acp-20-10125-2020, 2020.



Quelever, L. L. J., Kristensen, K., Jensen, L. N., Rosati, B., Teiwes, R., Daellenbach, K. R., Perakyla, O., Roldin, P., Bossi, R., Pedersen, H. B., Glasius, M., Bilde, M., and Ehn, M.: Effect of temperature on the formation of highly oxygenated organic molecules (HOMs) from alpha-pinene ozonolysis, *Atmos. Chem. Phys.*, 19, 7609-7625, 10.5194/acp-19-7609-2019, 2019.

Richters, S., Pfeifle, M., Olzmann, M., and Berndt, T.: endo-Cyclization of unsaturated RO₂ radicals from the gas-phase ozonolysis of cyclohexadienes, *Chem. Commun.*, 53, 4132-4135, 10.1039/c7cc01350g, 2017.

Rissanen, M. P., Kurten, T., Sipila, M., Thornton, J. A., Kangasluoma, J., Sarnela, N., Junninen, H., Jorgensen, S., Schallhart, S., Kajos, M. K., Taipale, R., Springer, M., Mentel, T. F., Ruuskanen, T., Petaja, T., Worsnop, D. R., Kjaergaard, H. G., and Ehn, M.: The Formation of Highly Oxidized Multifunctional Products in the Ozonolysis of Cyclohexene, *J. Am. Chem. Soc.*, 136, 15596-15606, 10.1021/ja507146s, 2014.

Rissanen, M. P., Kurten, T., Sipila, M., Thornton, J. A., Kausiala, O., Garmash, O., Kjaergaard, H. G., Petaja, T., Worsnop, D. R., Ehn, M., and Kulmala, M.: Effects of Chemical Complexity on the Autoxidation Mechanisms of Endocyclic Alkene Ozonolysis Products: From Methylcyclohexenes toward Understanding alpha-Pinene, *J. Phys. Chem. A* 119, 4633-4650, 10.1021/jp510966g, 2015.

Riva, M., Rantala, P., Krechmer, J. E., Perakyla, O., Zhang, Y. J., Heikkinen, L., Garmash, O., Yan, C., Kulmala, M., Worsnop, D., and Ehn, M.: Evaluating the performance of five different chemical ionization techniques for detecting gaseous oxygenated organic species, *Atmos. Meas. Tech.*, 12, 2403-2421, 10.5194/amt-12-2403-2019, 2019.

Rohrer, F., Bohn, B., Brauers, T., Bruning, D., Johnen, F. J., Wahner, A., and Kleffmann, J.: Characterisation of the photolytic HONO-source in the atmosphere simulation chamber SAPHIR, *Atmos. Chem. Phys.*, 5, 2189-2201, 2005.

Rollins, A. W., Kiendler-Scharr, A., Fry, J. L., Brauers, T., Brown, S. S., Dorn, H. P., Dube, W. P., Fuchs, H., Mensah, A., Mentel, T. F., Rohrer, F., Tillmann, R., Wegener, R., Wooldridge, P. J., and Cohen, R. C.: Isoprene oxidation by nitrate radical: alkyl nitrate and secondary organic aerosol yields, *Atmos. Chem. Phys.*, 9, 6685-6703, 2009.

Schwantes, R. H., Teng, A. P., Nguyen, T. B., Coggon, M. M., Crounse, J. D., St Clair, J. M., Zhang, X., Schilling, K. A., Seinfeld, J. H., and Wennberg, P. O.: Isoprene NO₃ Oxidation Products from the RO₂ + HO₂ Pathway, *J. Phys. Chem. A* 119, 10158-10171, 10.1021/acs.jpca.5b06355, 2015.

Skov, H., Hjorth, J., Lohse, C., Jensen, N. R., and Restelli, G.: Products and mechanisms of the reactions of the nitrate radical (NO₃) with isoprene, 1,3-butadiene and 2,3-dimethyl-1,3-butadiene in air, *Atmospheric Environment. Part A. General Topics*, 26, 2771-2783, [https://doi.org/10.1016/0960-1686\(92\)90015-D](https://doi.org/10.1016/0960-1686(92)90015-D), 1992.

Stark, M. S.: Epoxidation of Alkenes by Peroxyl Radicals in the Gas Phase: Structure-Activity Relationships, *The Journal of Physical Chemistry A*, 101, 8296-8301, 10.1021/jp972054+, 1997.

Stark, M. S.: Addition of Peroxyl Radicals to Alkenes and the Reaction of Oxygen with Alkyl Radicals, *J. Am. Chem. Soc.*, 122, 4162-4170, 10.1021/ja993760m, 2000.

Takeuchi, M., and Ng, N. L.: Chemical composition and hydrolysis of organic nitrate aerosol formed from hydroxyl and nitrate radical oxidation of alpha-pinene and beta-pinene, *Atmos. Chem. Phys.*, 19, 12749-12766, 10.5194/acp-19-12749-2019, 2019.

Tröstl, J., Chuang, W. K., Gordon, H., Heinritzi, M., Yan, C., Molteni, U., Ahlm, L., Frege, C., Bianchi, F., Wagner, R., Simon, M., Lehtipalo, K., Williamson, C., Craven, J. S., Duplissy, J., Adamov, A., Almeida, J., Bernhammer, A.-K., Breitenlechner, M., Brilke, S., Dias, A., Ehrhart, S., Flagan, R. C., Franchin, A., Fuchs, C., Guida, R., Gysel, M., Hansel, A., Hoyle, C. R., Jokinen, T., Junninen, H., Kangasluoma, J., Keskinen, H., Kim, J., Krapf, M., Kürten, A., Laaksonen, A., Lawler, M., Leiminger, M., Mathot, S., Möhler, O., Nieminen, T., Onnela, A., Petäjä, T., Piel, F. M., Miettinen, P., Rissanen, M. P., Rondo, L., Sarnela, N., Schobesberger, S., Sengupta, K., Sipilä, M., Smith, J. N., Steiner, G., Tomé, A., Virtanen, A., Wagner, A. C., Weingartner, E., Wimmer, D., Winkler, P. M., Ye, P., Carslaw, K. S., Curtius, J., Dommen, J., Kirkby, J., Kulmala, M., Riipinen, I., Worsnop, D. R., Donahue, N. M., and Baltensperger, U.: The role of low-volatility organic compounds in initial particle growth in the atmosphere, *Nature*, 533, 527-531, 10.1038/nature18271, 2016.

Valiev, R. R., Hasan, G., Salo, V.-T., Kubecka, J., and Kurten, T.: Intersystem Crossings Drive Atmospheric Gas-Phase Dimer Formation, *The journal of physical chemistry. A*, 123, 6596-6604, 10.1021/acs.jpca.9b02559, 2019.

Vereecken, L., and Peeters, J.: Nontraditional (per)oxy ring-closure paths in the atmospheric oxidation of isoprene and monoterpenes, *J. Phys. Chem. A* 108, 5197-5204, 10.1021/jp049219g, 2004.

Vereecken, L., Mueller, J. F., and Peeters, J.: Low-volatility poly-oxygenates in the OH-initiated atmospheric oxidation of alpha-pinene: impact of non-traditional peroxy radical chemistry, *Phys. Chem. Chem. Phys.*, 9, 5241-5248, 10.1039/b708023a, 2007.



Vereecken, L., and Peeters, J.: A structure-activity relationship for the rate coefficient of H-migration in substituted alkoxy radicals, *Phys. Chem. Chem. Phys.*, 12, 12608-12620, 10.1039/c0cp00387e, 2010.

Vereecken, L., and Francisco, J. S.: Theoretical studies of atmospheric reaction mechanisms in the troposphere, *Chem. Soc. Rev.*, 41, 6259-6293, 10.1039/c2cs35070j, 2012.

Vereecken, L., and Peeters, J.: A theoretical study of the OH-initiated gas-phase oxidation mechanism of beta-pinene (C₁₀H₁₆): first generation products, *Phys. Chem. Chem. Phys.*, 14, 3802-3815, 10.1039/c2cp23711c, 2012.

Vereecken, L., and Noziere, B.: H migration in peroxy radicals under atmospheric conditions, *Atmos. Chem. Phys.*, 20, 7429-7458, 10.5194/acp-20-7429-2020, 2020.

Wagner, N. L., Dubé, W. P., Washenfelder, R. A., Young, C. J., Pollack, I. B., Ryerson, T. B., and Brown, S. S.: Diode laser-based cavity ring-down instrument for NO₃, N₂O₅, NO₂ and O₃ from aircraft, *Atmos. Meas. Tech.*, 4, 1227-1240, 10.5194/amt-4-1227-2011, 2011.

Wennberg, P. O., Bates, K. H., Crounse, J. D., Dodson, L. G., McVay, R. C., Mertens, L. A., Nguyen, T. B., Praske, E., Schwantes, R. H., Smarte, M. D., St Clair, J. M., Teng, A. P., Zhang, X., and Seinfeld, J. H.: Gas-Phase Reactions of Isoprene and Its Major Oxidation Products, *Chem. Rev.*, 118, 3337-3390, 10.1021/acs.chemrev.7b00439, 2018.

Wu, R., Vereecken, L., Tsiligiannis, E., Kang, S., Albrecht, S. R., Hantzschke, L., Zhao, D., Novelli, A., Fuchs, H., Tillmann, R., Hohaus, T., Carlsson, P., Shenolikar, J., Bernard, F., Crowley, J. N., Fry, J. L., Brownwood, B., Thornton, J. A., Brown, S. S., Astrid, K.-S., Wahner, A., Hallquist, M., and Mentel, T. F.: Molecular composition and volatility of multi-generation 1 products formed from isoprene oxidation by nitrate radical, In preparation, 2020.

Xu, L., Guo, H. Y., Boyd, C. M., Klein, M., Bougiatioti, A., Cerully, K. M., Hite, J. R., Isaacman-VanWertz, G., Kreisberg, N. M., Knote, C., Olson, K., Koss, A., Goldstein, A. H., Hering, S. V., de Gouw, J., Baumann, K., Lee, S. H., Nenes, A., Weber, R. J., and Ng, N. L.: Effects of anthropogenic emissions on aerosol formation from isoprene and monoterpenes in the southeastern United States, *Proc. Nat. Acad. Sci. U.S.A.*, 112, 37-42, 10.1073/pnas.1417609112, 2015.

Zhao, D. F., Buchholz, A., Kortner, B., Schlag, P., Rubach, F., Kiendler-Scharr, A., Tillmann, R., Wahner, A., Flores, J. M., Rudich, Y., Watne, Å. K., Hallquist, M., Wildt, J., and Mentel, T. F.: Size-dependent hygroscopicity parameter (κ) and chemical composition of secondary organic cloud condensation nuclei, *Geophys. Res. Lett.*, 42, 10920-10928, 10.1002/2015gl066497, 2015a.

Zhao, D. F., Kaminski, M., Schlag, P., Fuchs, H., Acir, I. H., Bohn, B., Häsel, R., Kiendler-Scharr, A., Rohrer, F., Tillmann, R., Wang, M. J., Wegener, R., Wildt, J., Wahner, A., and Mentel, T. F.: Secondary organic aerosol formation from hydroxyl radical oxidation and ozonolysis of monoterpenes, *Atmos. Chem. Phys.*, 15, 991-1012, 10.5194/acp-15-991-2015, 2015b.

Zhao, D. F., Schmitt, S. H., Wang, M. J., Acir, I. H., Tillmann, R., Tan, Z. F., Novelli, A., Fuchs, H., Pullinen, I., Wegener, R., Rohrer, F., Wildt, J., Kiendler-Scharr, A., Wahner, A., and Mentel, T. F.: Effects of NO_x and SO₂ on the secondary organic aerosol formation from photooxidation of alpha-pinene and limonene, *Atmos. Chem. Phys.*, 18, 1611-1628, 10.5194/acp-18-1611-2018, 2018.

Ziemann, P. J., and Atkinson, R.: Kinetics, products, and mechanisms of secondary organic aerosol formation, *Chem. Soc. Rev.*, 41, 6582-6605, 10.1039/c2cs35122f, 2012.